Flow convergence routing hypothesis for pool-riffle maintenance in alluvial rivers

MacWilliams Jr., Michael L.; Wheaton, Joseph; Pasternack, Gregory P.; Street, Robert L.; Kitanidis, Peter K.

Published in:
Water Resources Research

DOI:
10.1029/2005WR004391

Publication date:
2006

Citation for published version (APA):
MacWilliams Jr., M. L., Wheaton, J., Pasternack, G. P., Street, R. L., & Kitanidis, P. K. (2006). Flow convergence routing hypothesis for pool-riffle maintenance in alluvial rivers. *Water Resources Research*, *42*(10). https://doi.org/10.1029/2005WR004391

WATER RESOURCES RESEARCH, VOL. 42, W10427, doi:10.1029/2005WR004391, 2006

Flow convergence routing hypothesis for pool-riffle maintenance in alluvial rivers

Michael L. MacWilliams Jr.,[1] Joseph M. Wheaton,[2,3] Gregory B. Pasternack,[3] Robert L. Street,[1] and Peter K. Kitanidis[1]

Received 29 June 2005; revised 28 April 2006; accepted 19 June 2006; published 31 October 2006.

[1] The velocity reversal hypothesis is commonly cited as a mechanism for the maintenance of pool-riffle morphology. Although this hypothesis is based on the magnitude of mean flow parameters, recent studies have suggested that mean parameters are not sufficient to explain the dominant processes in many pool-riffle sequences. In this study, two- and three-dimensional models are applied to simulate flow in the pool-riffle sequence on Dry Creek, California, where the velocity reversal hypothesis was first proposed. These simulations provide an opportunity to evaluate the hydrodynamics underlying the observed reversals in near-bed and section-averaged velocity and are used to investigate the influence of secondary currents, the advection of momentum, and cross-stream flow variability. The simulation results support the occurrence of a reversal in mean velocity and mean shear stress with increasing discharge. However, the results indicate that the effects of flow convergence due to an upstream constriction and the routing of flow through the system are more significant in influencing pool-riffle morphology than the occurrence of a mean velocity reversal. The hypothesis of flow convergence routing is introduced as a more meaningful explanation of the mechanisms acting to maintain pool-riffle morphology.

Citation: MacWilliams, M. L., Jr., J. M. Wheaton, G. B. Pasternack, R. L. Street, and P. K. Kitanidis (2006), Flow convergence routing hypothesis for pool-riffle maintenance in alluvial rivers, *Water Resour. Res.*, *42*, W10427, doi:10.1029/2005WR004391.

1. Introduction

[2] The velocity reversal hypothesis was introduced by *Keller* [1971] as a mechanism for understanding the maintenance of pool-riffle sequences in alluvial streams. This hypothesis was based on observations from Dry Creek, California, that "at low flow the bottom velocity is less in the pool than in the adjacent riffles" and that "with increasing discharge the bottom velocity in pools increases faster than in riffles" [*Keller*, 1971, p. 754]. The velocity reversal hypothesis proposes the removal of fine sediment from riffles into pools during low flows since velocity (or shear stress) is at a maximum over riffles [*Sear*, 1996]. As discharge rises, the velocity in pools increases and becomes greater than over riffles, resulting in a "velocity reversal." *Gilbert* [1914] first described this phenomenon noting that "at high stage ... the greater and smaller velocities have exchanged places," though it was *Keller* [1969, 1971] who first used the term 'velocity reversal' to describe this process. Since then, the velocity reversal hypothesis has initiated significant discussion in the literature and underlies a variety of conceptual models which attempt to describe the maintenance of pool-riffle morphology.

[3] Although Keller's proposal of the hypothesis focused on mean bottom velocities, subsequent studies have expanded the hypothesis to apply to mean boundary shear stress [*Lisle*, 1979], section-averaged velocity [*Keller and Florsheim*, 1993], and section-averaged shear velocity [*Carling*, 1991]. Other studies have focused on point measures of velocity and shear stress [*Petit*, 1987, 1990]. A brief synopsis of the primary studies which have addressed the velocity reversal hypothesis, including the type of study, the parameter evaluated, and our evaluation of the authors' support for the velocity reversal is given in the first three columns of Table 1. A more thorough discussion is presented by *MacWilliams* [2004].

[4] As seen in Table 1, the literature does not provide a clear consensus or single governing hypothesis for the mechanisms controlling pool-riffle morphology. Although there has been significant debate about whether a reversal of one or more flow parameters takes place, there is more general agreement that many cross-sectional average flow parameters in pools and riffles tend to converge as discharge increases [*Carling and Wood*, 1994]. While the literature suggests that a velocity reversal does occur in some cases, it is not clear whether a reversal of some type is a requisite for pool maintenance or whether the reversal hypothesis is applicable for all pool-riffle sequences. For example, *Clifford and Richards* [1992] found that a reversal or its absence could be demonstrated simultaneously for a given pool riffle sequence depending on the parameter evaluated, and the location of the measurement or cross section.

[1]Environmental Fluid Mechanics Laboratory, Department of Civil and Environmental Engineering, Stanford University, Stanford, California, USA.
[2]River Basin Dynamics and Hydrology Research Group, University of Wales, Aberystwyth, UK.
[3]Department of Land, Air, and Water Resources, University of California, Davis, California, USA.

0043-1397/06/2005WR004391$09.00

Table 1. Primary References Pertaining to the Velocity Reversal Hypothesis, With Our Best Assessment of the Type of Study, the Parameters Evaluated for a Reversal, and the Authors' Support for the Velocity Reversal and Flow Convergence Routing Hypotheses[a]

Reference	Type of Study	Reversal Parameter(s)	Support for Velocity Reversal	Support for Flow Convergence Routing
Keller [1969]	field	near-bed velocity	stated support	implied support
Keller [1970, 1971]	field	near-bed velocity	stated support	implied support
Keller [1972]	theoretical	N/A	not discussed	assumed support
Richards [1978]	1-d model	section average velocity and shear	inconclusive	not discussed
Lisle [1979]	field	mean shear stress	stated support	not discussed
Bhowmik and Demissie [1982]	field	N/A	negative	not discussed
Jackson and Beschta [1982]	field	near-bed velocity	stated support	assumed support
Lisle [1986]	field	N/A	not discussed	assumed support
Petit [1987, 1990]	field	point shear stress and velocity	inconclusive	assumed support
Carling [1991]	field	velocity, shear velocity	negative	implied support
Clifford and Richards [1992]	field	point and section-averaged velocity and shear stress	negative	implied support
Keller and Florsheim [1993]	1-D model	section average velocity	stated support	not discussed
Clifford [1993a, 1993b]	field	N/A	negative	assumed support
Carling and Wood [1994]	1-D model	section average velocity and shear velocity	conditional support	not discussed
Miller [1994]	2-D model	N/A	not discussed	assumed support
Sear [1996]	field, review	N/A	negative	not discussed
Thompson et al. [1996, 1998, 1999]	field, laboratory, 2-D model	Velocity	conditional support	assumed support
Booker et al. [2001]	3-D model	section average velocity, near-bed velocity, bed shear stress	conditional support	assumed support
Cao et al. [2003]	2-D model	bed shear stress, depth average velocity	conditional support	assumed support

[a]For the velocity reversal hypothesis, stated support indicates that the study supports the velocity reversal hypothesis for the case(s) analyzed; conditional support indicates that the study supported the velocity reversal under some conditions; inconclusive indicates that no firm statement of support or lack of support was made in the study; negative means the study rejected the hypothesis. For the flow convergence routing hypothesis, assumed support is applied to studies that explicitly discuss the significance of either a flow convergence or restriction for the study site(s), and it is assumed that these sites would support the flow convergence routing hypothesis; implied support applies to studies where these features were noted at the study site but not characterized as an important mechanism.

Support for a reversal hypothesis based on reversals in different types of flow parameters (as seen in Table 1) should be considered as a suite of multiple working hypotheses for explaining pool-riffle morphology rather than a single ruling hypothesis because different maintenance mechanisms may operate in different pool-riffle sequence. However, a review of all the published field data for sediment transport in pool-riffle sequences [*Sear*, 1996] has shown that a velocity or shear stress reversal does not explain all of the published evidence of sediment transport. Thus a more fundamental motivating question is that within systems that exhibit reversals of some kind, is the reversal an adequate explanation for pool maintenance? If not, and some alternative maintenance mechanism is hypothesized, can that alternative hypothesis explain pool maintenance in pool-riffle sequences that do not exhibit reversals?

[5] The extension of Keller's velocity reversal hypothesis from mean bottom velocity (as it was originally proposed) to section-averaged variables has been driven in part by the use of one-dimensional models to analyze pool-riffle sequences. *Keller and Florsheim* [1993] used a one-dimensional hydraulic model (HEC-RAS) to evaluate the velocity reversal hypothesis using Keller's original field data. They found that during high flows the mean pool velocity exceeded that of adjacent riffles, and that during low flows, the condition was reversed. Applying a similar model (HEC-2), *Carling and Wood* [1994] demonstrate the effect of varying channel width, riffle spacing, and channel roughness on the shear velocity, section mean velocity, and energy slope. However, in their results a reversal in the mean velocity took place only when the riffle was considerably wider than the pool. Similarly a "shear velocity reversal" took place only when the pool was rougher than the riffle. Both of these conclusions severely limit the conditions when a section-averaged velocity or shear velocity reversal could potentially occur and suggest that other mechanisms may be necessary to explain sediment transport in pool-riffle sequences. *Carling* [1991] found a convergence in mean velocity in pools and riffles in his study site, but concluded that riffles were not sufficiently wide at high flows to accommodate the known discharge with a velocity lower than in pools, and thus no velocity reversal was identified. Similarly, *Richards* [1978] found a narrowing of the difference in mean depth and velocity with discharge, but neither of these variables, nor surface slope or bed shear showed any tendency to equalize at the highest flow simulated. On the basis of their results, *Keller and Florsheim* [1993] concluded that more sophisticated models of the hydraulics associated with pool-riffle sequences will be able to explain in more detail the interaction between channel form and process in pool-riffle sequences in alluvial streams.

[6] There is a growing recognition that section-averaged data are not sufficient to explain the dynamics of pool-riffle sequences. Several studies have implemented two-dimensional models to simulate flow in pool-riffle sequences [e.g., *Miller*, 1994; *Thompson et al.*, 1998; *Cao et al.*, 2003]. Although *Miller* [1994] focused primarily on flow around a debris fan, his results identified the influence of flow convergence at the upstream end of the fan leading to the development of scour holes; thus his results demonstrate the importance of flow convergence in the formation of a riffle-pool sequence. Note that in this context "convergence" is used to define the physical process of funneling of flow rather than in the context of a narrowing difference between mean parameter values as it was used previously. Similarly, *Thompson et al.* [1998] identified the importance of a constriction at the head of the pool in creating a jet of locally high velocities in the pool center, and the formation of a recirculating eddy. *Cao et al.* [2003] found that at low discharge there exists a primary peak zone of bed shear stress and velocity at the riffle tail in line with the maximum energy slope, and a secondary peak at the pool head. With increasing discharge, the secondary shear stress peak at the head of the pool increases and approaches or exceeds the primary shear stress peak over the riffle. They also attributed the existence of a flow reversal in their simulation to the constriction at the pool head. *Booker et al.* [2001] applied a three-dimensional CFD model to a natural pool-riffle sequence. In their study, only three out of eight possible pool-riffle couplets experienced a mean velocity reversal. They found a tendency for near-bed velocity direction to route flow away from the deepest part of pools and suggest that this flow routing may have an important influence on sediment routing and the subsequent maintenance of pool-riffle morphology.

[7] Extensive field and laboratory observations have been made on the effects of flow constrictions on flow convergence and divergence, recirculating flow, and sediment routing. Constrictions resulting from debris fans [e.g., *Miller*, 1994; *Kieffer*, 1985, 1989; *Schmidt*, 1990] have been characterized by a flow regime consisting of a convergent flow upstream of the constriction, a beginning divergence out of the constrictions, and ultimately a downstream state of uniform flow not influenced by the constriction [*Kieffer*, 1985,1989]. *Schmidt* [1990] identifies the presence of a scour hole immediately downstream from most channel constrictions, and notes that recirculating currents can develop between the jet of flow exiting the constriction and the bank. *Thompson* [2004] has used laboratory experiments to investigate the influence of pool length on recirculating eddies and jet strength. Both *Thompson* [2004] and *Schmidt et al.* [1993] observed significant variation in instantaneous velocity field resulting in the recirculation zone, which indicates that average flow parameters are not sufficient to explain sediment transport. *Lisle and Hilton* [1992] observed nonuniform sediment deposition in pools which showed little correlation to water depth. They found that deposits were thickest under eddies and backwaters, but were commonly absent under the thalweg. Further, *Lisle and Hilton* [1992, p. 380] observed that "although some fine sediment is deposited in pools, boundary shear stress along the major sediment pathways in pools remained sufficient to maintain continued transport downstream." Similarly, *Jackson and Beschta* [1982] observed a nonuniform distribution of bedload transport across the channel resulting from a relatively large increase in velocity with discharge along the channel thalweg, with relatively little change in the lower velocities along the channel edges. This increase in velocity did not result in significant scour, but instead enabled bed material from the upstream riffle to be efficiently routed through the pool. These observations indicate that flow constrictions and a

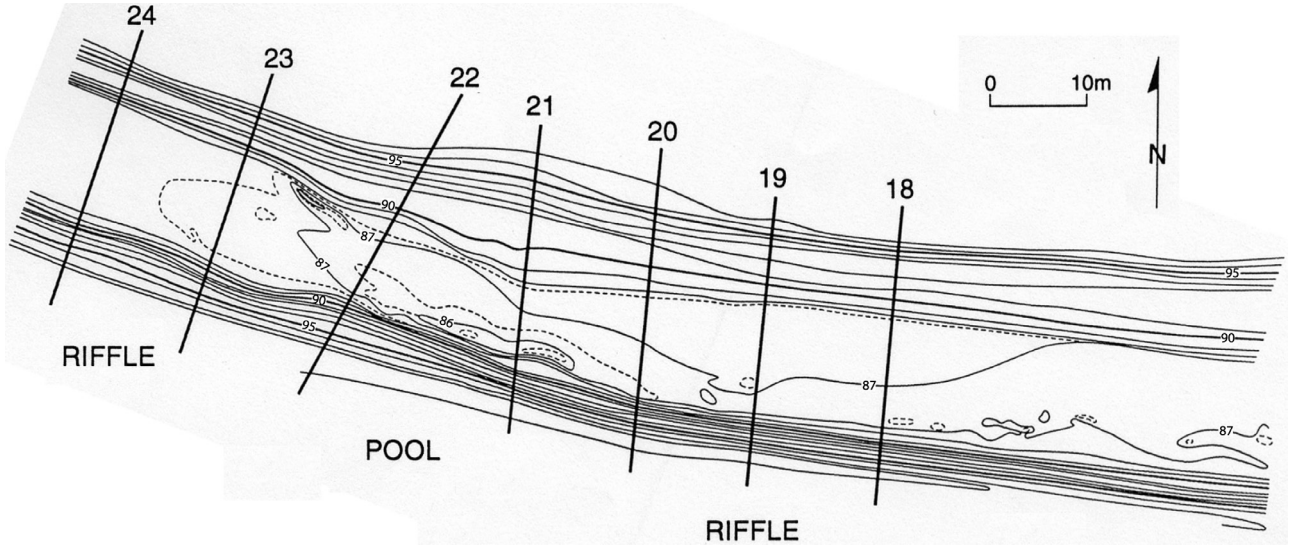

Figure 1. Topographic map of a riffle-pool-riffle sequence in Dry Creek near Winters, California. Contour interval is 1 foot (1 foot = 0.3048 m). Modified from *Keller and Florsheim* [1993]. Copyright 1993 John Wiley & Sons Limited. Reproduced with permission.

resulting nonuniform distribution of flow can have a significant impact on routing of sediment through pools.

[8] Drawing on this extensive literature, *Thompson et al.* [1996, 1998] have revised the traditional velocity reversal model to incorporate the effects of a channel constriction at the head of a pool. Their study demonstrated how the upstream constriction resulted in higher local velocities in the pool in comparison to adjacent riffles, despite a similar cross-sectional area. As noted by *Booker et al.* [2001], this concept links the concept of velocity reversal with work by *Keller* [1972] which suggested that the regular pattern of scour and deposition required for pools and riffles may be provided by an alternation of convergent and divergent flow patterns along the channel. This connection is significant because the pool-riffle sequence on Dry Creek has a point bar (on the north bank between sections 22 and 20 on Figure 1) which acts as constriction at the head of the pool. *Cao et al.* [2003] conclude that a channel constriction can, but may not necessarily, lead to [sediment transport] competence reversal, depending on channel geometry, flow discharge, and sediment properties. *Booker et al.* [2001] conclude that an analysis of near-bed velocity patterns suggested that the near-bed flow direction can cause routing of sediments away from the deepest part of the pools. Their results indicate maintenance of pool-riffle morphology by a lack of sediment being routed into pools rather than an increased ability to erode based on convergence of flow into the pool.

[9] The velocity reversal hypothesis was proposed by *Keller* [1971] based on bed velocity measurements in a pool-riffle sequence on Dry Creek, CA. The bed-velocity data [*Keller*, 1969, 1970] support a convergence of near-bed velocity, and a reversal in near-bed velocity is predicted for higher discharges. *Keller and Florsheim*'s [1993] one-dimensional modeling study support a reversal in mean velocity for the pool-rifle sequence on Dry Creek. The overall goal of this paper is to return to Keller's original data set to evaluate the flow processes in a pool-riffle sequence using two-dimensional and three-dimensional numerical simulations that may be able to explain the hydrodynamic mechanics underlying the observed conditions, which was not possible by previous one-dimensional simulation. Using both types of models not only provides a more complete assessment of the physical processes, but it also completes the systematic evaluation of the utility of different levels of process resolution. Specific objectives include (1) identifying pool-riffle "reversals" in near-bed velocity, depth-averaged velocity, section-averaged velocity, and bed shear stress, (2) evaluating the roles of secondary circulation and width constriction at the site, and (3) assessing whether the velocity reversal hypothesis is an adequate explanation for the maintenance of the pool-riffle morphology for this pool-riffle sequence. Although the study only investigates one site in detail, the hydrodynamic processes simulated in these models are transferable to other sites, and our analysis draws on both the extensive literature on pool-riffle morphology and experience on other rivers. On the basis of our analysis, a new "flow convergence routing" hypothesis for pool-riffle maintenance in alluvial rivers is proposed, which is consistent with Dry Creek conditions and those observed other sites reported in the literature. The new hypothesis is significant for its ability to explain why past studies on other field sites have differed in their assessment of the originally proposed velocity reversal mechanism.

2. Methods

[10] In this study, the Dry Creek reach mapped in Keller's original field study was modeled using both a two-dimensional and a three-dimensional hydrodynamic model. The models were validated using field data collected by *Keller* [1969] and compared against one-dimensional results from *Keller and Florsheim* [1993]. This approach allows for a detailed assessment of the capacity of one-, two- and three-dimensional models to capture the hydrodynamics and a strong basis for inference of important morphological processes that operate on this pool-riffle sequence. Specif-

ically, the one-dimensional results from *Keller and Florsheim* [1993] and the results from the two- and three-dimensional models applied in this study were used to assess whether a reversal in mean velocity occurred on Dry Creek. Further, the three-dimensional model was used to compare predicted bed velocity to the measurements from *Keller* [1971] and to evaluate whether a near-bed velocity reversal occurs, as Keller originally predicted. Lastly, the predicted bed shear stresses from the two- and three-dimensional simulations were used to evaluate whether a reversal in bed shear stress occurred and whether the spatial or temporal distribution of bed shear stresses indicate any other important mechanisms that could account for a reversal in sediment transport competence.

2.1. Two- and Three-Dimensional Modeling

[11] Two different numerical models were applied in this study. Although the two- and three-dimensional models were applied independently, to the extent possible, the model parameters used in the two- and three-dimensional simulations were equivalent to the model parameters used in the one-dimensional model presented by *Keller and Florsheim* [1993], to allow for a balanced comparison between the three models. The specific formulation of roughness, eddy viscosity, and boundary conditions were different in each model as described below, but the parameter values were calibrated to produce equivalent water surface elevations and cross-sectional area.

[12] Three-dimensional simulations were made using the three-dimensional nonhydrostatic hydrodynamic model for free surface flows on unstructured grids, UnTRIM, described by *Casulli and Zanolli* [2002]. The UnTRIM model solves the full three-dimensional momentum equations for an incompressible fluid under a free surface given by

$$\frac{\partial u}{\partial t}+u\frac{\partial u}{\partial x}+v\frac{\partial u}{\partial y}+w\frac{\partial u}{\partial z}-fv=-\frac{\partial p}{\partial x}+\nu^h\left(\frac{\partial^2 u}{\partial x^2}+\frac{\partial^2 u}{\partial y^2}\right)+\frac{\partial}{\partial z}\left(\nu^v\frac{\partial u}{\partial z}\right)$$

$$\frac{\partial v}{\partial t}+u\frac{\partial v}{\partial x}+v\frac{\partial v}{\partial y}+w\frac{\partial v}{\partial z}+fu=-\frac{\partial p}{\partial y}+\nu^h\left(\frac{\partial^2 v}{\partial x^2}+\frac{\partial^2 v}{\partial y^2}\right)+\frac{\partial}{\partial z}\left(\nu^v\frac{\partial v}{\partial z}\right)$$

$$\frac{\partial w}{\partial t}+u\frac{\partial w}{\partial x}+v\frac{\partial w}{\partial y}+w\frac{\partial w}{\partial z}=-\frac{\partial p}{\partial z}+\nu^h\left(\frac{\partial^2 w}{\partial x^2}+\frac{\partial^2 w}{\partial y^2}\right)+\frac{\partial}{\partial z}\left(\nu^v\frac{\partial w}{\partial z}\right)-g$$

where $u(x, y, z, t)$ and $v(x, y, z, t)$ are the velocity components in the horizontal x and y directions, respectively; $w(x, y, z, t)$ is the velocity component in the vertical z direction; t is the time; $p(x, y, z, t)$ is the normalized pressure defined as the pressure divided by a constant reference density; f is the Coriolis parameter; g is the gravitational acceleration; and ν^h and ν^v are the coefficients of horizontal and vertical eddy viscosity, respectively [*Casulli and Zanolli*, 2002]. Conservation of mass is expressed by the continuity equation for incompressible fluids

$$\frac{\partial u}{\partial x}+\frac{\partial v}{\partial y}+\frac{\partial w}{\partial z}=0.$$

The free surface equation is obtained by integrating the continuity equation over depth and using a kinematic condition at the free surface; this yields [*Casulli and Zanolli*, 2002]

$$\frac{\partial \zeta}{\partial t}+\frac{\partial}{\partial x}\left[\int_{-H^0}^{\zeta} u dz\right]+\frac{\partial}{\partial y}\left[\int_{-H^0}^{\zeta} v dz\right]=0,$$

where $h(x, y)$ is the prescribed bathymetry measured downward from the reference elevation and $\eta(x, y, t)$ is the free surface elevation measured upward from the reference elevation. Thus the total water depth is given by $H(x, y, t) = h(x, y) + \eta(x, y, t)$. The discretization of the above equations and model boundary conditions is presented in detail by *Casulli and Zanolli* [2002] and is not reproduced here. The UnTRIM model was modified to include an inflow boundary condition for volume and momentum, a radiation outflow boundary condition, and a modified formulation of bed drag and vertical eddy viscosity as described by *MacWilliams* [2004].

[13] The two-dimensional finite element surface water modeling system (FESWMS) was used to analyze depth-averaged hydrodynamics following the approach of *Pasternack et al.* [2004]. FESWMS solves the vertically integrated conservation of momentum and mass equations using a finite element method to acquire depth averaged 2D velocity vectors and water depths at each node in a finite element mesh. The model is capable of simulating both steady and unsteady two-dimensional flow as well as subcritical and supercritical flows. The basic governing equations for vertically integrated momentum in the x and y directions under the hydrostatic assumption are given by

$$\frac{\partial}{\partial t}(HU)+\frac{\partial}{\partial x}(\beta_{uu}HUU)+\frac{\partial}{\partial y}(\beta_{uv}HUV)+gH\frac{\partial z_b}{\partial x}+\frac{1}{2}g\frac{\partial H^2}{\partial x}+\frac{1}{\rho}\left[\tau_x^b-\frac{\partial}{\partial x}(H\tau_{xx})-\frac{\partial}{\partial y}(H\tau_{xy})\right]=0$$

and

$$\frac{\partial}{\partial t}(HV)+\frac{\partial}{\partial x}(\beta_{vu}HVU)+\frac{\partial}{\partial y}(\beta_{vv}HVV)+gH\frac{\partial z_b}{\partial y}+\frac{1}{2}g\frac{\partial H^2}{\partial y}+\frac{1}{\rho}\left[\tau_y^b-\frac{\partial}{\partial x}(H\tau_{yx})-\frac{\partial}{\partial y}(H\tau_{yy})\right]=0,$$

respectively, where H is the water depth, U and V are the depth-averaged velocity components in the horizontal x and y directions, z_b is the bed elevation, β_{uu}, β_{uv}, β_{vu}, and β_{vv} are the momentum correction coefficients that account for the variation of velocity in the vertical direction, τ_x^b and τ_y^b are the bottom shear stresses acting in the x and y directions, respectively, and τ_{xx}, τ_{xy}, τ_{yx} are the τ_{yy} shear stresses caused by turbulence. Conservation of mass in two dimensions is given by

$$\frac{\partial H}{\partial t}+\frac{\partial}{\partial x}(HU)+\frac{\partial}{\partial y}(HV)=0.$$

Discretization of the above equations for the FESWMS model is presented by *Froehlich* [1989], and is not reproduced here.

[14] The bathymetry for the Dry Creek field site [*Keller*, 1969] was digitized from a plane table survey contour map to generate a Digital Elevation Model (DEM) of the study reach in Autodesk's LandDesktop R3 Terrain Manager (Figure 1). The refined DEM data was then exported and interpolated onto each of the model grids. The total reach modeled is approximately 135 m long and ranges in width between 20 and 25 m. The FESWMS model used a finite element mesh with an approximately uniform node spacing of 0.45 m. This resulted in a model mesh with roughly 12,600 computational nodes comprising approximately 3500 mixed quadrilateral and triangular elements. For the UnTRIM model, an unstructured horizontal grid consisting of 23,655 cells triangular in planform was developed using TRIANGLE [*Shewchuk*, 1996]. The average grid cell size was 0.12 m^2. The seven cross sections in the study reach (Figure 1) were preserved in the model grids by aligning the edges of the model grid cells along the section lines. This facilitated direct comparison of model results with Keller's field data at specific cross sections. A uniform vertical grid spacing of 0.05 m was used for the UnTRIM simulations.

[15] *Keller* [1971] found that at low flow the Manning's *n* roughness coefficient in the pool-riffle sequence was 0.040 for the pool and 0.042 for the riffle. *Keller and Florsheim* [1993] used a roughness of 0.041 over pools and 0.043 over riffles in their simulations. *Keller and Florsheim* [1993] did a sensitivity analysis of bottom roughness by comparing their results using these values to a case where the roughness values were reversed and a case where a roughness of 0.041 was used in both the riffles and pools, and found no change in the relative velocities in the pools and riffles. They found that relative velocities are more dependent on channel geometry than on variation in roughness. Specification of bed roughness in a two- and three-dimensional model requires a spatially distributed roughness specified at each grid point, rather than coefficient at each cross section. In addition, this parameter represents only the effect of bed roughness, rather than encompassing all forms of energy loss in the channel as it does in a one-dimensional model. In the FESWMS model and the UnTRIM model, the bed roughness value is the principal calibration parameter used to calibrate the water surface slope. As a result, the bed roughness values were selected such that the predicted water surface matched the observed water surface. Because a detailed mapping of roughness for the Dry Creek site was not available, a constant roughness parameter was applied in both the FESWMS and the UnTRIM simulations. In the FESWMS simulations the Manning's *n* roughness was estimated as 0.041 for entire study site. For the UnTRIM simulations a constant z_o roughness of 1.5×10^{-3} m was applied. On the basis of the method described by *MacWilliams* [2004], this roughness height corresponds to a Manning's *n* value of approximately 0.041 for the range of flow depths simulated. The results from the UnTRIM and FESWMS simulations suggest that the roughness values selected primarily influence the water surface slope, and that the primary flow features are controlled by the channel geometry. Although local variations in roughness are likely to influence local shear stress values and bed velocity values, the large-scale flow features observed in this study are primarily controlled by the geometry of the pool-riffle sequence. This corroborates *Keller and Florsheim*'s [1993] conclusion that relative velocities are more dependent on channel geometry than on variation in roughness.

[16] For the FESWMS simulations, Boussinesq's analogy was applied to parameterize eddy viscosity, which crudely approximates eddy viscosity as an isotropic scalar. Doing so allows a theoretical estimate of eddy viscosity as 60 percent of the product of shear velocity and depth [*Froehlich*, 1989]. A constant eddy viscosity value of 0.027 m^2/sec was used for all FESWMS model runs. It is well known that the eddy viscosity has a nearly parabolic distribution with depth in an open channel flow and that the use of a constant eddy viscosity for three-dimensional simulations is likely to yield unrealistic vertical velocity profiles [*Rodi*, 1993]. As a result, in uniform open channels, the velocity profile is often assumed to be logarithmic, resulting in a parabolic eddy viscosity distribution [*Celik and Rodi*, 1988]. For the UnTRIM simulations, a parabolic vertical eddy viscosity model was applied following the approach of *Celik and Rodi* [1988].

[17] Keller's original field measurements [*Keller*, 1969, 1971] were made at discharges of 0.42, 0.97, and 4.5 m^3/s. The HEC-RAS model simulations by *Keller and Florsheim* [1993] were conducted for five steady flow rates, including the three discharges measured by *Keller* [1969] and two larger discharges of 8.5 and 17 m^3/s. These five flow rates were modeled as five separate steady flow simulations in FESWMS; in UnTRIM a transient simulation of each flow rate was run until the flow field reached a "steady state." In both UnTRIM and FESWMS, the inflow discharge was specified at the upstream end of the channel using a uniform velocity distribution; at the downstream end of the channel, the water surface elevation was specified based on the elevations predicted at the downstream cross section from the modeled results of *Keller and Florsheim* [1993]. To allow direct comparison with previous studies, we evaluated the model results at the pool cross section (section 19, Figure 1) and riffle cross section (section 21, Figure 1) used in the analysis of *Keller* [1971] and *Keller and Florsheim* [1993].

2.2. Model Validation

[18] The UnTRIM and FESWMS models have previously been validated in a number of applications [cf. *Casulli and Zanolli*, 2002; *MacWilliams*, 2004; *Froehlich*, 1989; *Pasternack et al.*, 2004]. For this application, the models were validated using field data collected by *Keller* [1969] to the extent possible recognizing the technological limitations and differing purpose of the original work. Validation of detailed numerical models against historical field data poses a significant challenge, because only sparse data are available for validation purposes. At the Dry Creek field site, the primary objective of the data collection effort was for the bed load movement experiments reported by *Keller* [1969, 1970], and only limited point velocity and water surface elevation data are available. Bed velocity measurements were made at the pool cross section (section 21) and riffle cross section (section 19) for 0.42, 0.97, and 4.5 m^3/s discharges. Velocity was also measured at 0.6 times the depth for the 0.42 and 0.97 m^3/s discharges. Observed cross-sectional areas for the pool and riffle cross sections were reported by *Keller and Florsheim* [1993], while observed depths at these cross sections are available only for the 0.97 m^3/s discharges (E. A. Keller, unpublished field

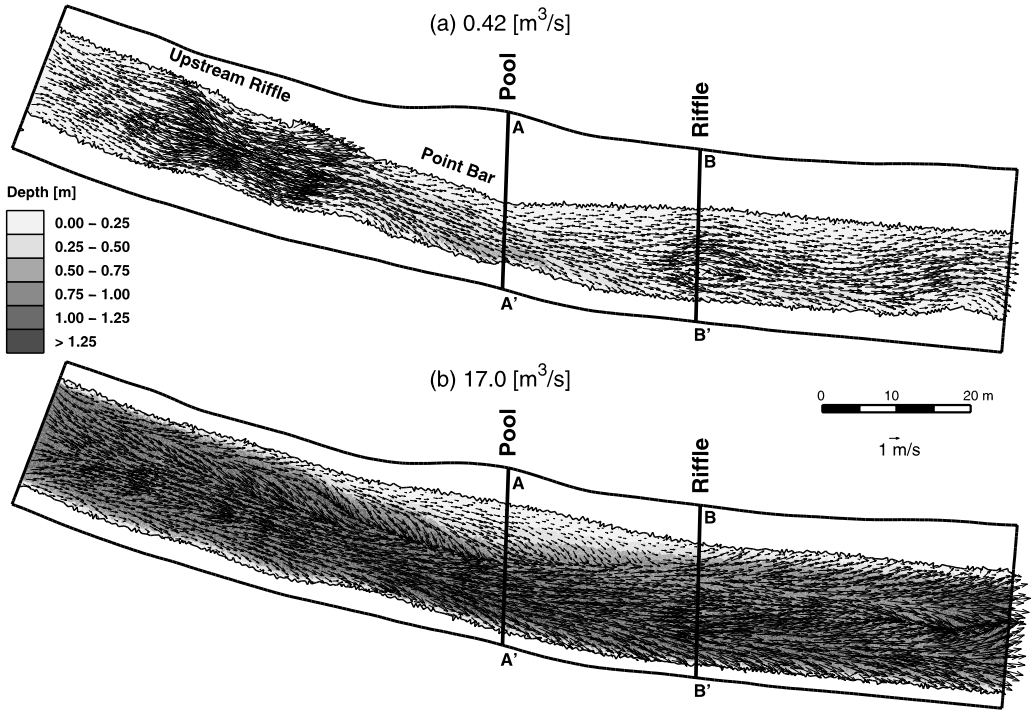

Figure 2. Predicted surface velocity vectors and depth on Dry Creek for (a) 0.42 and (b) 17.0 m^3/s flow rates. Surface velocities are shown for a subset of the UnTRIM computational cells.

notebook, 1969). The stations where these point data were collected are measured along each cross section but the exact starting position for each transect is not precisely reported; the alignment used was estimated using water surface edges and depths where available. While more detailed data collection using modern instruments would allow for more thorough model validation, we recognize that the available data was collected for a different purpose, and with relatively little quality control. Where the model results deviate from the available data, multiple data types have been used to help understand these differences. These comparisons highlight some potential shortcomings in the available data, and suggest that, while a reasonable level of validation can be achieved, some remaining differences may result from uncertainty in available observation data rather than model uncertainty.

2.3. Bed and Depth-Averaged Velocity

[19] On the basis of bed velocity measurements on Dry Creek, *Keller* [1971] predicted the occurrence of a bed velocity reversal. *Keller* [1969] believed that the "bottom velocity is much more significant in analyzing bed load movement than the mean velocity of the entire stream." Keller collected velocity measurements near the bed at three foot intervals along each of four cross sections during measured discharges of 0.42, 0.97, and 4.5 m^3/s. Velocities near the bed were measured with at rod-mounted, pigmy Price current meter [*Keller*, 1970]. For comparison with the bottom velocity measured by Keller, the velocity predicted using UnTRIM in the bottom two cells in each water column was interpolated to estimate the average velocity at a depth of 5 cm. On the basis of the geometry of the instrument used, this seems to be a reasonable estimate of the lowest height at which the velocity could feasibly be sampled. Because the pigmy Price current meter method does not measure flow direction and assumes all flow is in one direction, the overall velocity magnitude predicted by UnTRIM is used rather than only the downstream flow component. This distinction is significant for areas in which significant secondary circulation exists near the channel bed. Comparisons of bed velocity were not made using the FESWMS results, since FESWMS is a depth-averaged model. Depth-averaged velocities from FESWMS were compared to velocities measured at 0.6 times the depth for the 0.42 and 0.97 m^3/s discharges.

2.4. Section-Averaged Velocity

[20] *Keller and Florsheim* [1993] extended *Keller*'s [1969] original proposal of a reversal in bed velocity to a reversal in mean cross-section velocity. In their analysis, the field measurements from *Keller* [1969] were averaged over the pool and riffle cross sections and HEC-RAS was used to model section-averaged velocity. In this study, the predicted flow fields from FESWMS and UnTRIM at the pool and riffle cross sections were also averaged at the pool and riffle cross sections to obtain the cross-sectional average velocities for each of the five flow rates. These average velocities were compared to the results presented by *Keller and Florsheim* [1993].

2.5. Bed Shear Stress

[21] The predicted bed shear stress was calculated over the model domain for both the UnTRIM and FESWMS simulations. For the FESWMS simulations, the depth-averaged shear stress was calculated from depth, velocity, and bed roughness using a drag force relation [*Froehlich*, 1989]. Bed shear stress for the FESWMS simulation was calculated as 0.51 times the depth-averaged shear stress based on a detailed validation study (*Pasternack et al.*, submitted for

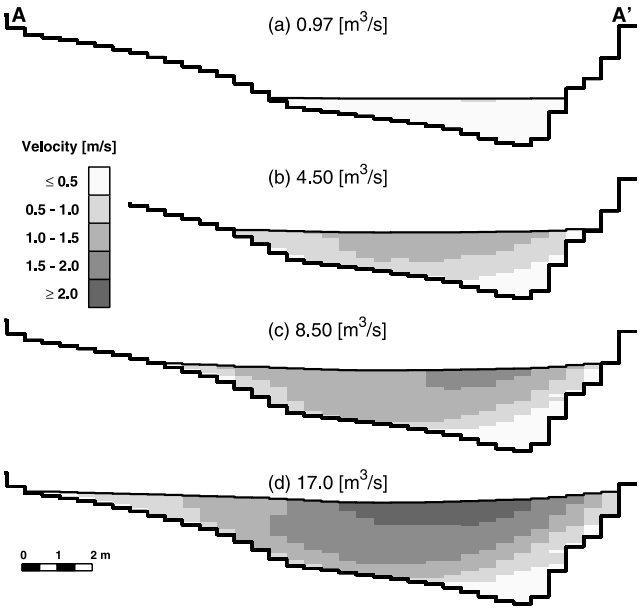

Figure 3. Downstream velocities at pool cross section predicted using UnTRIM for five flow rates. Cross sections are shown with 2 times vertical exaggeration.

publication, 2005). In the UnTRIM simulations, the bed shear stress was calculated from the near-bed velocity by assuming a log law near the bed [*MacWilliams*, 2004].

3. Results

[22] The predicted surface velocity and flow depth from the UnTRIM simulation for the 0.42 and 17.0 m^3/s discharges are shown in Figure 2. At a discharge of 0.42 m^3/s the highest surface velocities are predicted over the riffle upstream of the pool cross section and over the riffle cross section. The pool cross section is significantly narrower than the upstream riffle or the downstream riffle due to the point bar, and there is little variation of surface velocity across the pool cross section. The flow width increases downstream of the point bar, and flow is diverted around a local topographic high near the riffle cross section. Downstream of the riffle cross section the flow is more uniform. At a discharge of 17.0 m^3/s, the flow is fairly uniform across the upstream riffle but there is a noticeable deflection of surface velocities away from the shallow portions of the point bar as the flow approaches the pool cross section. The point bar is flooded, but low surface velocities are predicted in the shallower areas on the point bar; the highest predicted surface velocities at the pool cross section occur within a narrow zone midway across the section. As seen in Figure 2, the pool cross section widens more with discharge than the riffle cross section, such that at the 17.0 m^3/s discharge the flow width is relatively uniform over the entire reach; the shallow channel margins on the riffle cross section are much smaller than on the pool cross section. The predicted downstream velocities from the UnTRIM simulation at the pool cross section (section 21) are shown in Figure 3. The highest velocities occur near the surface, and the flow tends to be concentrated in the center section of the pool, with the highest velocities near the bed occurring over the point bar side of the pool rather than in the deepest section of the pool. This effect becomes more pronounced at higher discharges. Downstream of the pool, the flow diverges as the width of the point bar decreases; flow is more uniform across the channel the at the riffle cross section and further downstream.

3.1. Water Surface Elevation

[23] The water surfaces predicted at the pool and riffle cross sections for the UnTRIM and FESWMS simulations are compared with the observed water surfaces in Figure 4. Because observed water surface elevations were not available, the observed water surface was calculated at each discharge from the observed cross-sectional areas at the pool and riffle cross sections reported by *Keller and Florsheim* [1993] using the cross section geometries shown in Figure 4. At the pool cross section, the FESWMS and UNTRIM simulations predict a water surface approximately 0.07 to 0.08 m higher than the observed water surface for the 0.42 m^3/s discharge and 0.06 to 0.08 m lower than the observed water surface for the 0.97 m^3/s discharge. For the 4.5 m^3/s discharge, the UnTRIM simulation predicts a water surface within 0.01 m for most of the flow width, while the FESWMS simulation predicts a slightly higher water surface. At the riffle cross section, the water surface elevations predicted using both FESWMS and UnTRIM differ from the observed values by less than 0.02 m for all three flow rates for which observed data are available. For the 0.97 m^3/s discharge, depth measurements are available at the stations where velocity was measured (E. A. Keller, unpublished field notebook, 1969). The depth measurements are reported to an accuracy of 0.03 m (0.1 ft). These measurements of depth are plotted upward from the pool topography on Figure 4. These measurements show a large scatter (0.27 m between the maximum and minimum "observed" depth), which suggests variation between the local bathymetry where the measurement was taken and the bathymetry from the plane table survey topography used in this study. A similar level of scatter is also seen when the observed depths are plotted at the riffle cross section. The observed depths at the pool cross section show better agreement with the water surface predicted by UnTRIM and FESWMS than the observed water surface calculated from the observed cross-sectional area. The average elevation of the observed depths plotted for the 0.97 m^3/s discharge differs by less than 0.02 m from the average elevation predicted by both FESWMS and UnTRIM. This suggests that the water surfaces predicted for this discharge are reasonable, and that there may be some reliability uncertainties with the observed cross-sectional area at the pool cross section. Namely, the model cross sections were derived from topographic data from a plane table survey whereas the observed cross sections are approximately located on this survey and collected with a separate hand-level survey. Additionally, the original calculation of flow area was from a limited number of depth collection stations, variations between the surveyed topography and the stations where data was collected exist, and errors are introduced by back calculating the water depth from the reported observed cross-sectional area. Despite these potential sources of error, very good agreement between observed and predicted water surfaces are achieved at the riffle cross section for all three

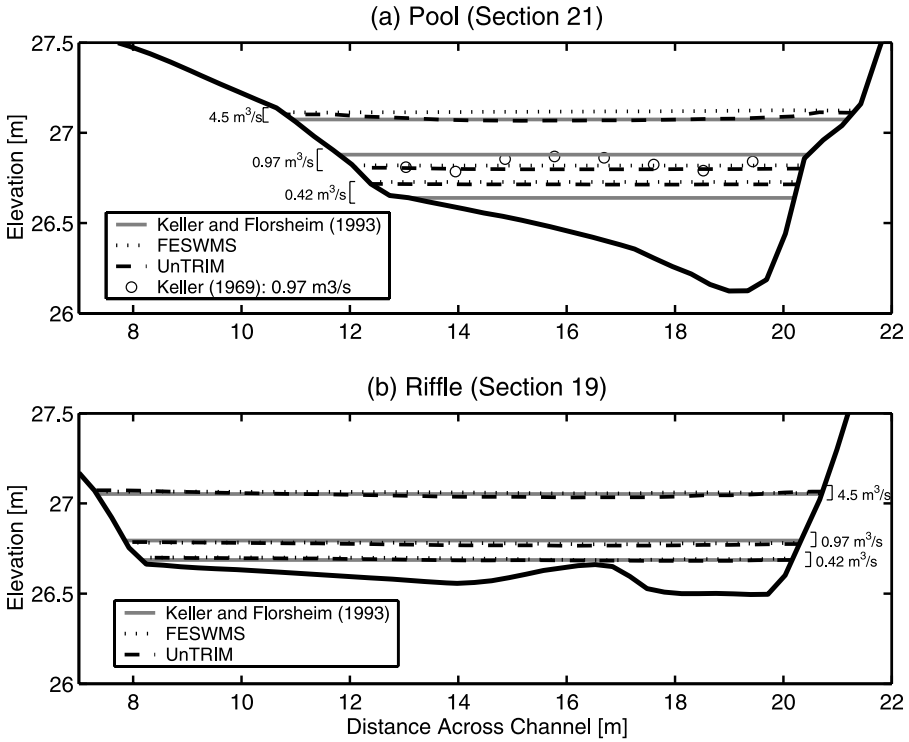

Figure 4. Predicted and observed water surface elevations at the (a) pool and (b) riffle cross sections for 0.42, 0.97, and 4.5 m^3/s discharges.

discharges, and reasonable agreement is achieved at the pool cross section.

3.2. Bed and Depth-Averaged Velocity

[24] The bed velocity measurements at the pool and riffle cross sections are compared with the predicted near-bed velocity from UnTRIM on Figures 5 and 6, respectively. There is generally good agreement between the measured bed velocity and the bed velocity predicted by UnTRIM at the pool cross section for each of the three discharges at which data was collected (Figure 5). No data were collected in the deepest part of the pool for the 4.5 m^3/s flow rate because the water was too deep and swift to collect measurements (E. A. Keller, unpublished field notebook, 1969). At all three discharges, the maximum measured and maximum predicted bed velocity at the pool cross section does not occur in the deepest part of the pool.

[25] For the riffle cross section, shown in Figure 6, there is also very good agreement between the measured and modeled bed velocity for each of the three discharges at which data was collected. The biggest observed difference between the field observations and the model predictions occurs on the right margin of the riffle cross section for a discharge of 4.5 m^3/s. As will be discussed below, this area of the riffle cross section exhibits significant secondary circulation at a discharge of 4.5 m^3/s and higher; for these discharges the predicted cross-stream velocity component near the bed is of a comparable magnitude to the downstream velocity component in this portion of the riffle. This flow complexity, and any unsteadiness associated with these flow patterns, appears to be the primary mechanism responsible for the difference between the predicted and observed bed velocity on the right edge of the riffle cross section. However, overall the simulation results show good agreement with the field observations at the riffle cross section. The agreement between the predicted and measured bed velocity at both the pool and riffle sections for the three discharges at which data is available indicates that the UnTRIM model is accurately simulating flow in Dry Creek at these discharges.

[26] The velocity measurements collected at 0.6 times the depth at the pool and riffle cross sections are compared with the predicted depth-averaged velocity from FESWMS on Figures 7. At the pool cross section the predicted depth-averaged velocity agrees well with the observed velocity at 0.6 times the depth for the 0.42 m^3/s discharge except at a distance of 14 m along the section where velocities were observed to be zero. For the 0.97 m^3/s discharge FESWMS slightly overpredicts velocities between 12 and 14 m along the section, and slightly under predicts velocity between 18 and 20 m. At the riffle cross section, the velocities predicted for the 0.42 m^3/s discharge show good agreement with observed velocities, while FESWMS consistently predicts lower velocities than the observed velocities at the 0.97 m^3/s. Differences between the observed velocity and the depth-averaged velocity predicted by FESWMS may result from the assumption that the velocity at 0.6 times the depth is equivalent to the depth-averaged values. For example, since the observed and predicted water surface and cross-sectional area at the riffle cross section (Figure 4) is nearly identical and the flow rates are identical, consistently higher observed depth-averaged velocities at the 0.97 m^3/s discharge is not consistent with continuity. Given this limitation in assuming that the velocity at 0.6 times the depth is equivalent to the depth-averaged values, the depth-

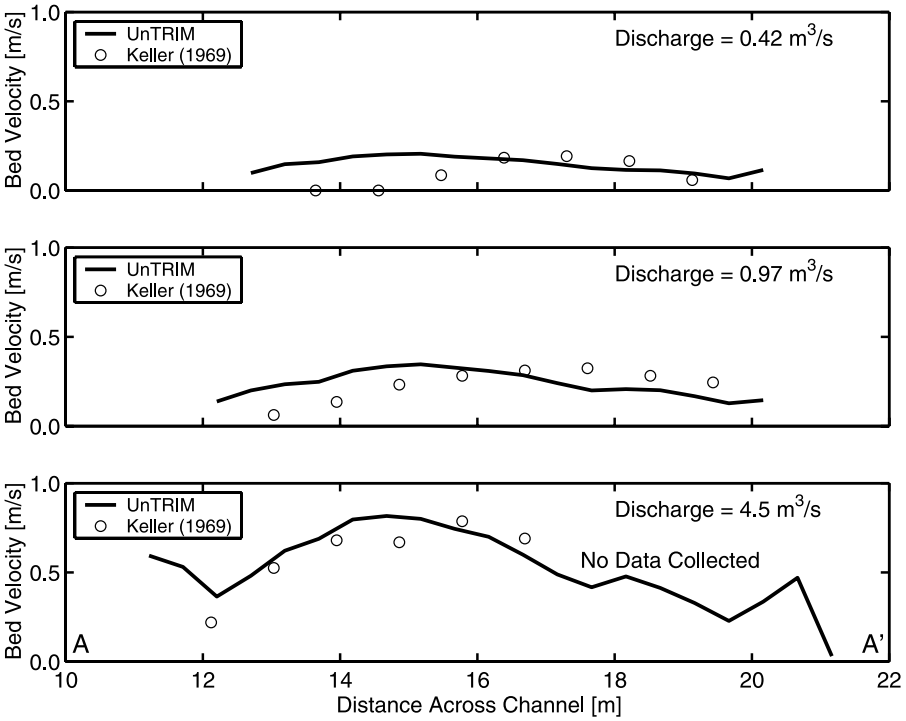

Figure 5. Predicted and observed near-bottom velocity at pool cross section for 0.42, 0.97, and 4.5 m^3/s discharges.

averaged velocities predicted by FESWMS show a reasonable agreement with the observed values.

3.3. Section-Averaged Velocity

[27] The predicted cross-sectional average velocities at the pool and riffle cross sections are shown as a function of discharge in Figure 8. For all flows, the HEC-RAS model [*Keller and Florsheim*, 1993] predicted a somewhat lower mean velocity (larger cross-sectional area) at the riffle cross section than the 2-D and 3-D models, with the largest differences occurring for the lower discharges. The 2-D and 3-D models show better agreement with the field data

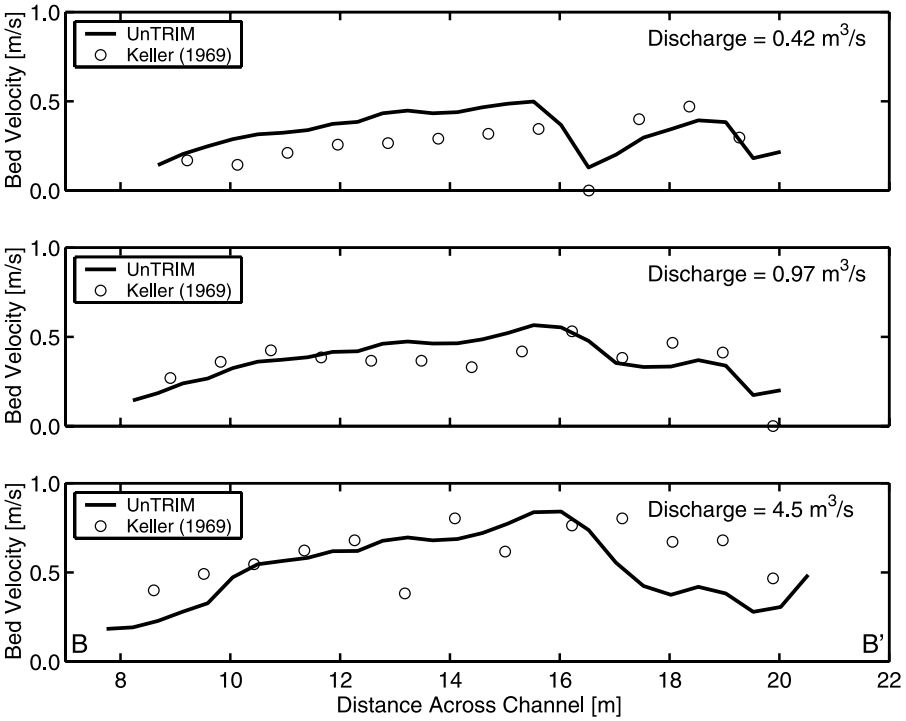

Figure 6. Predicted and observed near-bottom velocity at riffle cross section for 0.42, 0.97, and 4.5 m^3/s discharges.

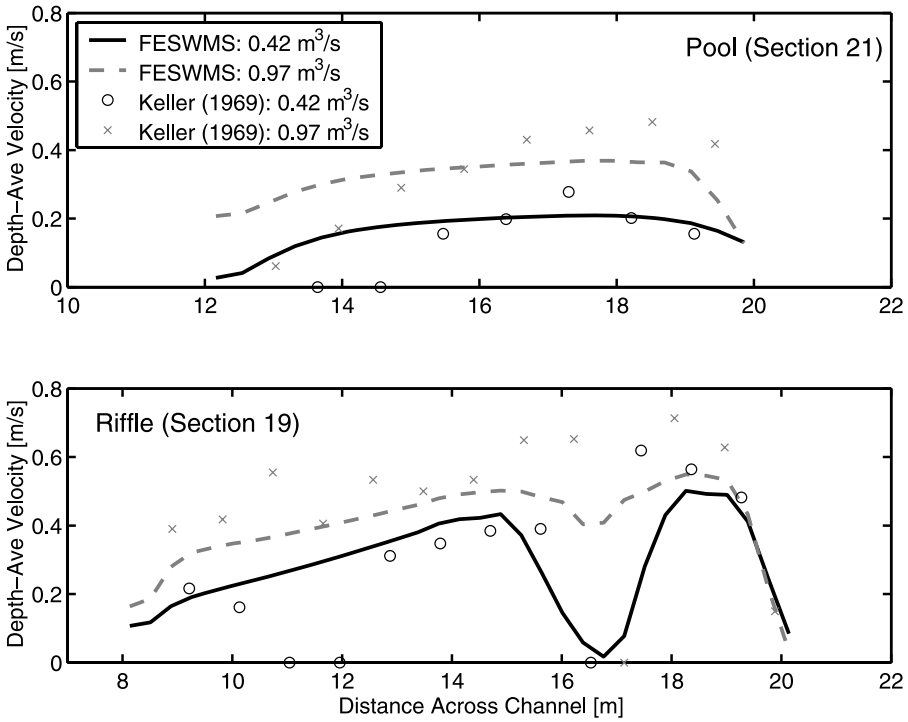

Figure 7. Observed velocity at 0.6 times the depth and predicted depth average velocity from FESWMS and for 0.42 and 0.97 m^3/s discharges at the (a) pool and (b) riffle cross sections.

for the riffle cross section. At the pool cross sections, all three models consistently underpredict the cross-sectional average velocity relative to the observed value at the 0.42 m^3/s discharge, and overpredict the cross-sectional average velocity at the 0.97 m^3/s discharge. All three models show good agreement with the observed cross-sectional average velocity at the pool cross section for the 4.5 m^3/s discharge. This is consistent with the differences in predicted and observed cross-sectional area at the pool cross section shown in Figure 4. Using HEC-RAS, *Keller and Florsheim* [1993] predicted a reversal in mean velocity at approximately 3.3 m^3/s. The FESWMS (2-D) simulation

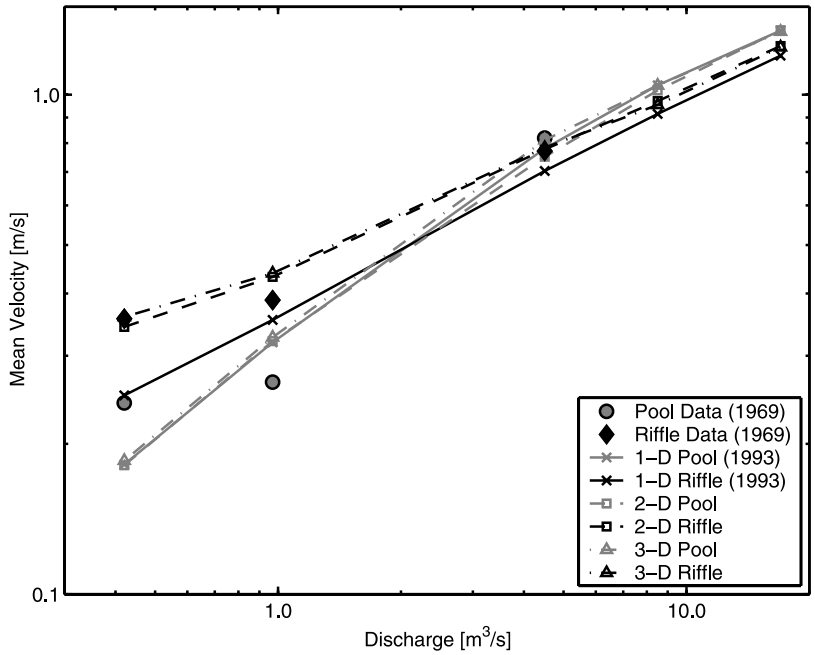

Figure 8. Mean cross-section velocity as a function of discharge at pool and riffle cross sections from field measurements [*Keller*, 1969] and predicted using a 1-D model [*Keller and Florsheim*, 1993], 2-D model (FESWMS), and 3-D model (UnTRIM).

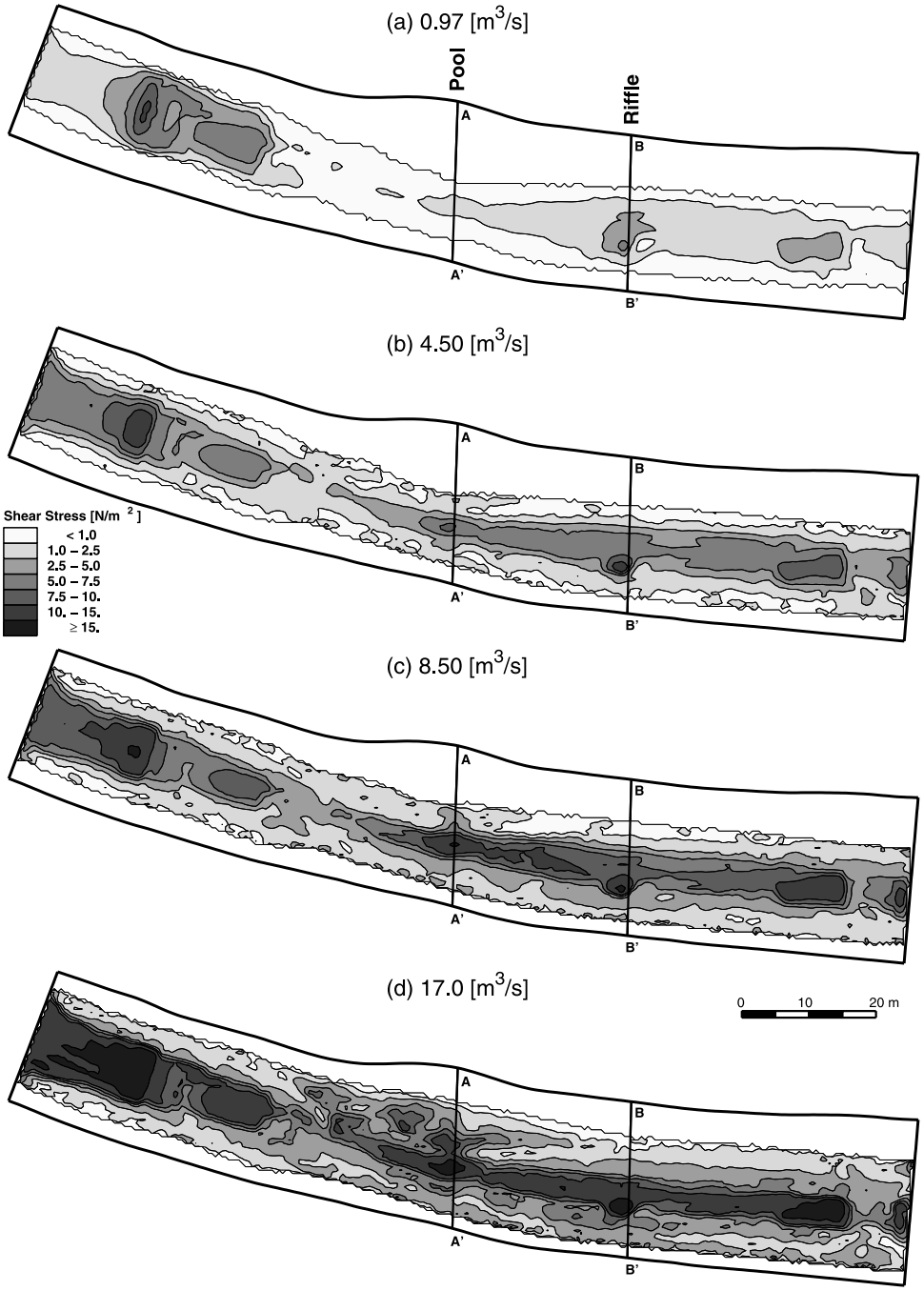

Figure 9. Bed shear stress distribution for four flow rates on pool-riffle sequence on Dry Creek from UnTRIM simulations.

predicts a reversal in cross-sectional average velocity at approximately 5.9 m^3/s, and the UnTRIM (3-D) simulation results predict a reversal in mean cross-sectional velocity at a discharge of approximately 3.8 m^3/s. This analysis shows that all three models predict a reversal in cross-sectional average velocity for this pool-riffle sequence on Dry Creek.

3.4. Bed Shear Stress

[28] Planform maps of bed shear stress for four of the five discharges simulated from the UnTRIM and FESWMS simulations are shown in Figures 9 and 10, respectively. For the 0.97 m^3/s flow (Figures 9a and 10a) the UnTRIM and FESWMS simulations predict a similar distribution of shear stress, with the highest shear stresses occurring over the upstream riffle and a narrower zone of high shear stresses through the pool cross section which widens downstream over the riffle cross section. This zone of higher shear stress along the center of the channel becomes more pronounced with increasing discharge. The UnTRIM simulations predict a more distinct band of higher shear stresses along the center of the channel with lower shear stresses along the channel margins (and in the deepest part of the pool). The shear stress distribution predicted by the FESWMS simulations shows a more uniform distribution of

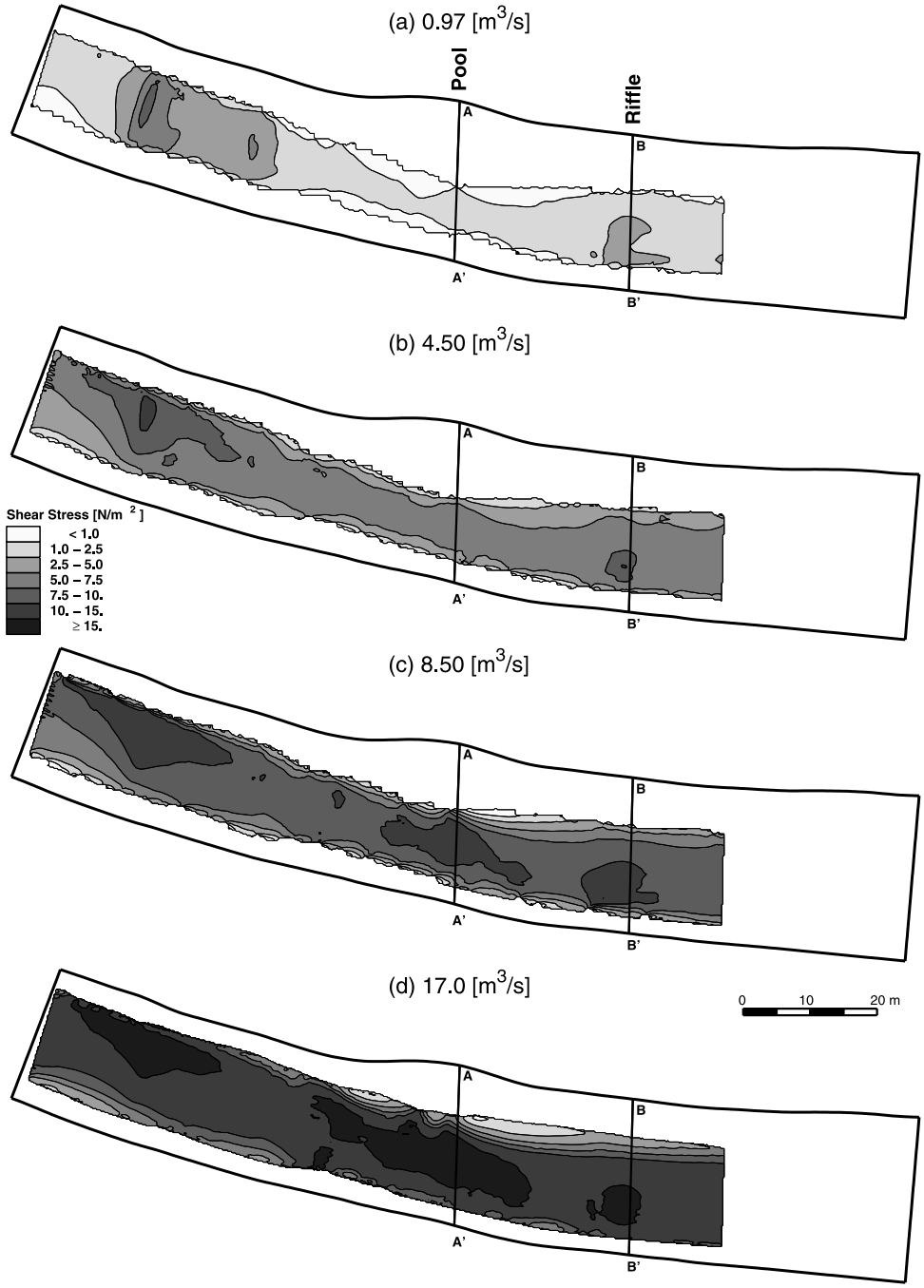

Figure 10. Bed shear stress distribution for four flow rates on pool-riffle sequence on Dry Creek from FESWMS simulations (the modeled reach for the FESWMS simulations was shorter than for the UnTRIM simulations but is shown on the same scale to facilitate comparison).

shear stresses across the channel, but still show the highest shear stresses concentrated in the center of the channel. As with the near-bed velocity (Figure 5), the maximum bed shear stresses predicted at the pool cross section occur on the slope of the point bar, rather than in the deepest part of the pool for both models and at all discharges. At the riffle cross section, the bed shear stress at the lower two flow rates is fairly uniform across the channel, with the highest values occurring near the middle of the cross section and at a local topographic high point (e.g., Figure 4). In general, the bed shear stresses predicted from the FESWMS simulations (Figure 10) tend to be slightly higher than the bed shear stresses predicted from the 3-D UnTRIM simulations (Figure 9). This discrepancy results from calculating the bed shear stress from the depth-averaged velocity rather than the near-bed velocity. However, these comparative results confirm the practical utility of scaling the depth-averaged shear stress predictions by a factor of 0.51 to yield a reasonable estimate of bed shear stress.

[29] The bed shear stresses shown in Figure 9 were averaged over the pool and rifle cross sections. Figure 11 shows the cross-sectional average and cross section maxi-

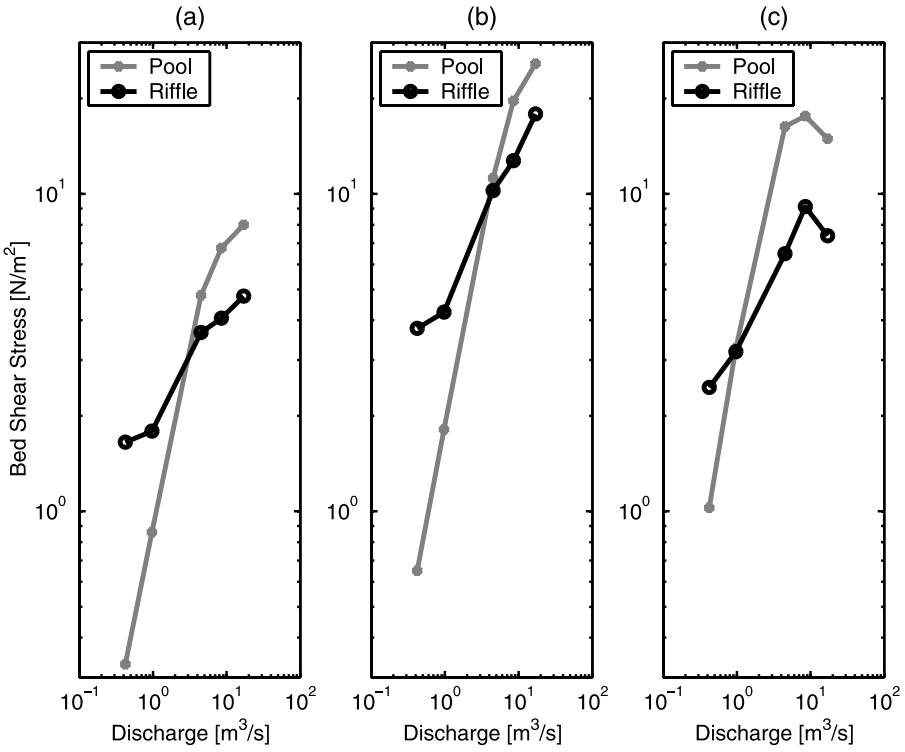

Figure 11. Bed shear stress as a function of discharge at the pool and riffle cross sections: (a) Section average bed shear stress predicted using UnTRIM. (b) Section maximum bed shear stress predicted using UnTRIM. (c) Bed shear stress calculated using the depth-slope product for pool and riffle cross sections using depth and water surfaces from UnTRIM simulations.

mum shear stresses at the pool and riffle cross sections predicted using UnTRIM. The shear stress predicted by applying the depth-slope product at the pool and riffle cross sections is also shown for comparison. A reversal in cross-sectional averaged bed shear stress occurs at a discharge of 3.0 m^3/s and a reversal in maximum cross-section bed shear stress occurs at a discharge of 3.9 m^3/s. The shear stresses predicted using the depth-slope product show a reversal at a discharge of 0.94 m^3/s.

3.5. Secondary Circulation

[30] Although the analysis of cross-sectional average parameters provides a relatively simple metric for analyzing flow processes, cross-sectional average parameters do not reliably account for flow complexity in systems where significant secondary circulation exists. Figure 12 shows the magnitude and direction of the cross-stream flow component along the pool cross section (section 21) for four of the five discharges studied. As seen in Figure 12, significant secondary circulation cells develop at the pool cross section for the discharges of 4.5 m^3/s and greater. The degree of secondary circulation predicted at the pool cross section increases significantly with discharge. At the 0.42 (not shown) and 0.97 m^3/s flow rates, a single small secondary circulation cell is visible in the deepest part of the pool. As the discharge increases, the magnitude of the transverse velocities increases significantly and a separate weaker circulation cell develops over the shallow section of the point bar. These results are consistent with field observations made by Keller at the Dry Creek site. His field observations suggest there is considerably more turbulence at high flows in pools than in adjacent point bars and that some pools in Dry Creek appear to be formed by "vertical vortexes" scouring the pool bottom [*Keller*, 1969]. By "vertical vortices" it is assumed that Keller is referring to the large vertical circulation cells visible in Figure 12 at higher discharges. These circulation cells are also likely to play a significant role in mobilizing sediments in the deepest portion of the pool as discharge increases. It should also be noted that in general the secondary flow at the pool cross section shows a dominant flow direction from left to right. This tendency becomes more pronounced as discharge increases, especially near the surface over the point bar where the downstream velocities are largest. This effect indicates that the cross-section line is not exactly perpendicular to the primary flow direction (cross-section location on Figure 1; flow direction on Figure 2). However, since this cross-section alignment was used by *Keller* [1969, 1971] and *Keller and Florsheim* [1993], this alignment is maintained in this study. Figure 13 shows the magnitude and direction of the cross-stream flow component along the riffle cross section for four of the five discharges studied. At the 0.97 m^3/s discharge, a small circulation cell is visible on the right side of the cross section. The magnitude of this circulation cell increases significantly with increasing discharge. A second weaker eddy is visible on the left side of the cross section for discharges of 4.5 m^3/s and greater.

4. Discussion

4.1. Bed Velocity

[31] Keller's original bed velocity measurements showed a convergence rather than a reversal in mean bed velocity;

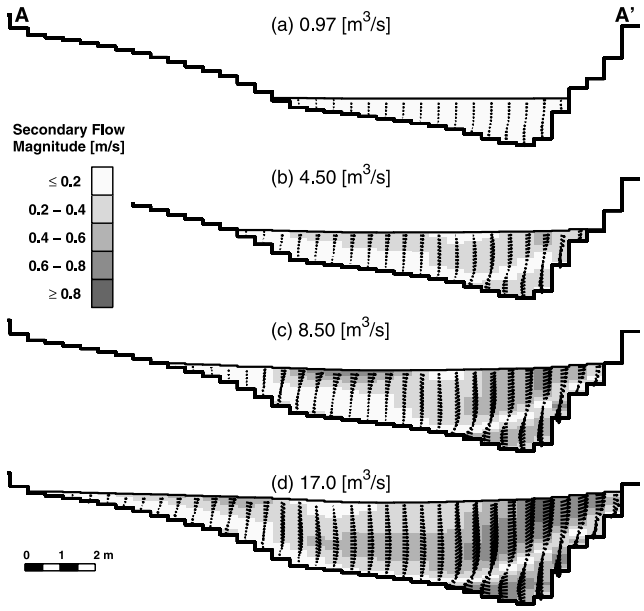

Figure 12. Secondary flow magnitude and direction at pool cross section A-A′ predicted using UnTRIM for five flow rate. Cross sections are shown with 2 times vertical exaggeration.

however, *Keller* [1969, 1971] postulated that a reversal in mean bed velocity would occur at a discharge above 4.5 m^3/s. By averaging the near-bed velocity at the pool and riffle cross sections for each of the five flow rates, it is possible to determine whether a reversal in mean near-bed velocity occurs in Dry Creek. The UnTRIM simulations predict a reversal in mean cross-section bed velocity at approximately 4.0 m^3/s and a reversal in maximum cross-section bed velocity at approximately 5.1 m^3/s. The consideration of the maximum bed velocity is significant because it is the locally maximum bed velocity in the cross section rather than the cross-sectional average value which gives a better indication of the local sediment transport competence. A reversal in mean bed velocity occurred prior to a reversal in maximum bed velocity, while the predicted reversal in mean bed velocity occurred at a slightly lower discharge than was predicted by *Keller* [1971]. However, these results support *Keller*'s [1971] original prediction that a reversal in near-bed velocity would occur on his pool-riffle study site on Dry Creek.

4.2. Section-Averaged Velocity

[32] A velocity reversal refers to the discharge at which the cross-sectional average velocity at the pool cross section exceeds the cross-sectional average velocity at the riffle cross section. Because the instantaneous discharge in both cross sections is identical, a reversal in mean cross-section velocity corresponds identically with a reversal in mean cross-sectional area. This reversal in cross-section area is largely a function of the site geometry. Through a systematic modeling study using a 1-D model, *Carling and Wood* [1994] found that a reversal in mean cross-section velocity only took place when the riffle was considerably wider than the pool. In their study, the ratio of pool to riffle width did not vary as a function of discharge. In contrast, at the Dry Creek field site, the riffle is approximately 50% wider than the pool at a flow rate of 0.42 m^3/s, but then only 25% wider than the pool at a flow rate of 4.5 m^3/s, and slightly narrower than the pool at a discharge of 17.0 m^3/s (e.g., Figure 9). The widening of the pool at a higher rate with increasing discharge in this case served as the geometric mechanism that led to a reversal in cross-sectional area and thus a reversal in section-averaged velocity. Depending on the absolute values of width and depth at low flow in an adjacent pool and riffle, the trajectory in changes in those variables that leads to a reversal in cross-sectional area can be quite different. Thus the particular trajectory observed in Dry Creek should not be viewed as a unique solution leading to a velocity reversal.

4.3. Bed Shear Stress

[33] *Carling and Wood* [1994] found that a "shear velocity reversal" took place whenever the pool had a significantly higher roughness coefficient than the riffle, but under no other conditions. In their study, the shear velocity, U_*, was calculated as

$$U_*^2 = gdS,$$

where g is gravity, d is the average water depth, and S is the energy slope. On the basis of this equation, commonly referred to as the depth-slope product, a higher value of the shear velocity is highly dependent on the energy slope. The average predicted cross-sectional depth and water surface slope (as a proxy for energy slope) at the pool and riffle cross sections from the UnTRIM simulations were used to calculate the shear velocity using this equation. The simulation results showed a significant variation in water surface elevation and downstream water surface slope along the cross section, making the calculation of a meaningful cross-sectional average energy slope difficult. As a result, the average water surface slope was calculated over a 10 m reach centered on the pool and riffle cross sections. The average depth of the riffle was less than the average depth of

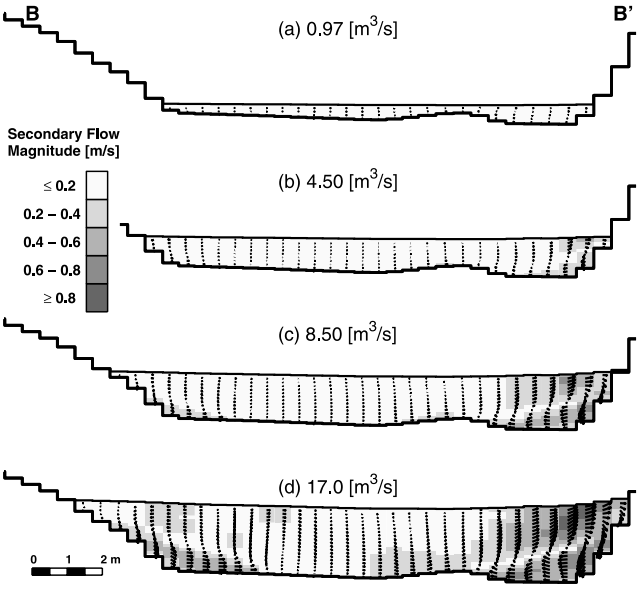

Figure 13. Secondary flow magnitude and direction at riffle cross section B-B′ predicted using UnTRIM for five flow rates. Cross sections are shown with 2 times vertical exaggeration.

the pool for the discharges less than 17.0 m^3/s, but greater than the average depth of the pool for a discharge of 17.0 m^3/s. This reversal in average depth occurs due to the widening of the pool onto the shallow areas of the point bar with increasing discharge (seen in Figure 2), whereas the riffle width does not increase as significantly with discharge. At the riffle cross section, the increase in flow depth with discharge is more pronounced than the increase in width. The water surface slope at the riffle cross section decreases with discharge; the water surface at the pool cross section steepens with discharge for the first three discharges and then decreases in slope for higher discharges. The difficulty associated with calculating a representative average water surface slope increases with discharge because the water surface elevation along and across the cross section becomes more complex at higher discharges. Thus there is a significant degree of uncertainty in the estimates of water surface slope at higher discharges. Applying the average depth and water surface slope parameters to the above equation predicts a reversal in bed shear stress at a discharge of 0.94 m^3/s. This result is not consistent with the predicted mean and maximum bed shear stresses shown in Figure 11. Similarly, the shear stress maps shown on Figure 9 and 10 do not support the drop in shear stress at the pool and riffle cross sections for the highest discharge, as is predicted by the application of the depth-slope product.

[34] This analysis of shear velocity using a one-dimensional approach illustrates the inappropriateness of applying one-dimensional equations to flows where significant cross-stream flow patterns are evident. In flows where significant two- and three-dimensional flow patterns are significant, one-dimensional step backwater models (such as HEC-RAS) do not provide a reliable estimate of friction slope and the slope-depth product does not yield a reliable estimate of shear velocity. *Thompson et al.* [1996] have argued that water surface slope is of little use in the calculation of shear stresses in systems where complex wave patterns and localized flow conditions influence longitudinal water surface slopes. In addition, variations in water surface elevation along a given cross section also lead to a range of possible water surface slopes between two given cross sections [*Miller*, 1994]. These factors all suggest that a one-dimensional approach is not appropriate for estimating bed shear stress in this pool-riffle sequence.

[35] A comparison of the predicted shear stresses from the FESWMS and UnTRIM simulations (Figures 9 and 10) provides insight into the relative importance of three-dimensional flow processes in predicting bed shear stress on Dry Creek. As mentioned above, one of the important mechanisms identified by the UnTRIM simulation is the convergence of the highest shear stresses into a narrow zone of flow routing through the channel. A qualitative comparison of Figures 9 and 10 shows that the width of higher shear stresses relative to the overall width of the channel is much narrower in the UnTRIM simulation than the FESWMS simulations. Part of this difference results because the secondary circulation cells on both margins of the channel (Figures 12 and 13) act to enhance the concentration of the flow in the center of the channel. Additionally the use of a horizontal eddy diffusivity in the FESWMS model acts to smooth out the horizontal velocity gradients, thereby reducing cross-stream flow variability. These conclusions are supported by additional 2-D simulations made using UnTRIM which show less flow convergence than the 3-D UnTRIM simulations, but more flow convergence than the FESWMS simulations. This effect could be reduced in the FESWMS simulations by using a spatially distributed eddy viscosity.

4.4. Secondary Circulation

[36] *Clifford and Richards* [1992, p. 67] have argued that "the interaction of channel form and channel flow at any point within a riffle-pool unit depends in part on flow and sediment behavior in upstream and downstream units," and that "if anything, explanations relying on cross-sectional averages complicate, rather than clarify, the characteristics of flow and form interaction." *Clifford and Richards* [1992] base this argument in part on the difficulty in accurately calculating the energy slope in the presence of complex secondary flow, and conclude that in the presence of a complex secondary flow the application of a 1-D equation of the form of equation discussed above is unacceptable. The results presented in the previous section, which demonstrate the significant secondary circulation patterns at both the pool and riffle cross sections, and the apparent inconsistencies found when applying the depth-slope equation to the range of flows simulated on Dry Creek, support this conclusion.

4.5. Flow Constriction

[37] *Keller* [1969] found that the at-a-point maximum bottom velocities at the pool cross section (Figure 5) showed a tendency for the highest velocities to be located on the point bar side of the pool rather than in the center of the pool. His bottom velocity measurements suggest that the area of high bottom velocity is "never in the center of the pool" and that "with increasing velocity there is a tendency for the area of high bottom velocity to migrate toward the point bar side of the pool" [*Keller*, 1969]. This feature is also observed in the shear stress distribution predicted by the UnTRIM simulations shown in Figure 9. The highest near-bed velocities, and thus the highest bed shear stresses, occur on the point bar and not in the deepest part of the pool. The alignment of this area of high flow velocity and shear stress with the flow constriction upstream of the pool on Dry Creek suggest that the upstream flow constriction is playing an important role in flow routing through the pool cross section.

[38] To test the influence of the upstream constriction on the velocity and shear stress distribution in the pool cross section on Dry Creek, an additional UnTRIM simulation was made with a modified numerical method that neglects the advective acceleration terms in the three-dimensional model. In effect, this approach removes any potential effects resulting from the flow convergence associated with the constriction at the head of the pool. The velocity distribution at the pool cross section for the simulation which neglects advective acceleration, shown in Figure 14, shows a dramatically different velocity distribution than was observed in the simulation results shown in Figure 3. For the simulation without advective acceleration, the maximum velocities and shear stresses occur over the deepest part of the pool instead of over the point bar as was observed by *Keller* [1969] and seen in the simulation results presented in the previous section. This result shows that the constriction

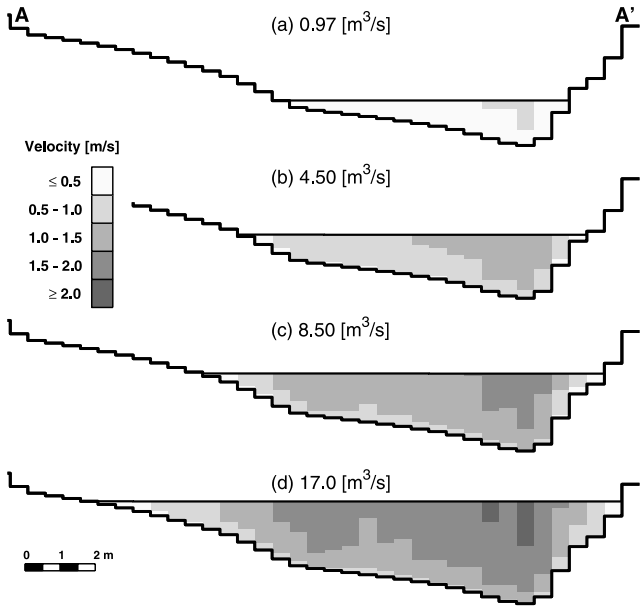

Figure 14. Downstream velocities at pool cross section for five flow rates predicted by UnTRIM simulation without advective acceleration. Cross sections are shown with 2 times vertical exaggeration.

at the head of the pool on Dry Creek is having a significant impact on the hydrodynamics of the pool-riffle sequence on Dry Creek. It also demonstrates that models that do not incorporate the full complexity of three-dimensional hydrodynamics and advective acceleration cannot accurately predict the important flow processes that occur in the pool-riffle sequence on Dry Creek. This result supports the results of *Whiting and Deitrich* [1991] which show that convective acceleration terms are important where topographic forcing leads to significant cross-stream and downstream flow accelerations. Another interesting outcome of this simulation without advective acceleration is that the results still predict a reversal in mean velocity at a discharge of 4.5 m^3/s. This result supports the conclusion that the occurrence of a mean velocity reversal is controlled more by the relative width of the pool and riffle than by the dominant flow processes in the pool-riffle sequence.

4.6. Flow Convergence Routing

[39] *Clifford and Richards* [1992] concluded that there is a need to formulate explanations of the maintenance of pool-riffle sequences that are sensitive to local variation and the existence of spatially distributed form process feedbacks. The results of the three-dimensional simulations of the pool-riffle sequence on Dry Creek support this conclusion. While the simulation results support a reversal in mean velocity, mean bed velocity, mean bed shear stress, and a variety of other cross-sectional average parameters, a reversal in mean parameters is not sufficient to explain the geomorphic processes that are necessary to maintain the pool-riffle sequence on Dry Creek. Fundamentally, this is because a reversal in mean velocity is not, in and of itself, sufficient to explain the important mechanisms occurring in the pool-riffle sequence on Dry Creek. A reversal in mean velocity does not explain the occurrence of the high velocities observed on the point bar rather than in the deepest part of the pool and it does not explain the important effects that advective acceleration have on the distribution of predicted velocities in the pool cross section. While a velocity reversal, or a convergence of cross-sectional average flow parameter values is observed in many pool-riffle sequences, there is a significant body of evidence in the literature that suggests that more complicated flow processes are significant in the maintenance of pool-riffle morphology. The flow complexity evident in almost all field studies and every two- and three-dimensional modeling study of pool-riffle sequences to date indicate that one-dimensional parameters and one-dimensional models are not adequate to capture the flow complexity in pool-riffle sequences. As a result, it is a reasonable conclusion that a hypothesis for pool-riffle morphology based on cross-sectional average parameters is not appropriate for explaining all of the processes important for maintaining pool-riffle morphology.

[40] A working hypothesis for defining the important processes for maintaining pool-riffle morphology can be introduced based on the processes observed on Dry Creek. It is called here the hypothesis of 'flow convergence routing' and is thought to be a more meaningful mechanism for explaining the key processes maintaining the pool-riffle morphology in Dry Creek than the occurrence of a velocity reversal. The hypothesis draws on elements of the work of *Booker et al.* [2001] and *Thompson et al.* [1996, 1998], but considers the maintenance mechanisms more explicitly. Under this hypothesis, the formation and maintenance of a pool depends on the occurrence of an upstream flow constriction which results in a convergence and acceleration of flow at the head a pool; this effectively generates a jet of flow through and downstream of the constriction. The effect of this convergence increases with discharge, and results in the development of a zone of high velocity and shear stress along a well-defined zone within the channel. Near bed flow is routed through this zone of high velocity resulting in high shear stress; this zone of high velocity and shear stress is the primary pathway for sediment movement through the pool. This zone of flow routing corresponds to the highest near-bed velocities, shear stresses, and maximum particle size. This zone is the primary pathway for sediment routing through the pool and can serve to route the coarsest sediment away from the deepest part of the pool. The lateral variation of flow along the edge of the convergence zone creates a lateral shear between the faster moving water over the point bar and the slower moving water over the deeper portion of the pool. This lateral shear zone has a significant impact on the secondary circulation pattern observed at the pool cross section, and this circulation plays a role in mobilizing sediment in the deepest part of the pool. Depending on the geometry of the site, a separation zone and recirculating eddy may also develop. At the tail of the pool, the flow diverges at the head of the riffle leading to deposition on the riffle and the maintenance of a topographic high at the tail of the pool. This hypothesis of flow convergence routing can explain how hydrodynamic processes evident in Dry Creek result in maintenance of the pool-riffle sequence, is supported by the data and observations of *Keller* [1969], and is supported by the results of other studies of pool-riffle sequences.

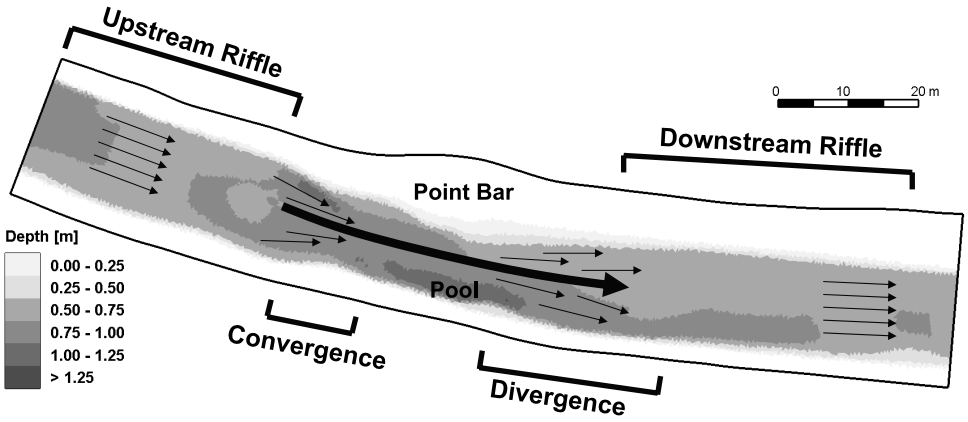

Figure 15. Conceptual model of flow convergence routing for pool-riffle sequence on Dry Creek. Depths shown for 4.5 m^3/s discharge.

[41] A conceptual model of the flow convergence routing mechanism during high flows on Dry Creek is shown in Figure 15. At the upstream riffle, the flow is fairly uniform across the channel. The point bar at the pool cross section acts as a constriction, and the flow is concentrated over a smaller width of channel. This funneling of flow results in a zone of higher velocity and sediment transport competence (depicted by wide dark arrow) that acts to route flow and sediment through the pool reach. Downstream of the point bar, the flow diverges and spreads out over the downstream riffle. At a sufficient distance downstream of the constriction, the flow on the downstream riffle is again fairly uniformly distributed across the riffle.

[42] The introduction of the flow convergence routing hypothesis is not a rejection of the results of *Keller* [1969, 1971]. Rather, the introduction of a more detailed hypothesis is a recognition that cross-sectional average parameters are not sufficient to explain the important processes in maintaining pool-riffle morphology. However, *Keller* [1969] also identified the significance of flow convergence routing on Dry Creek. He observed that "the point bar, which is slightly upstream, also tends to converge water into the pool. This is not significant at low flow, but may be important in producing fast bottom velocities at high flow. Water coming out of the pool diverges on the riffle, and this is probably responsible for the slower bottom velocity in the riffle at high flow." Further, Keller concluded that "it is assumed that at high flow the convergence of the pool produces fast bottom velocity which has a jetting action on the bed material; when the material reaches the divergent and slower bottom velocity of the riffle, the coarser material may be dropped from the moving traction load."

[43] The occurrence of flow routing in Dry Creek is also supported by Keller's observations that the highest velocities in the pool tended to be located on the point bar side of the pool rather than in the center of the pool. The bedload movement experiments on Dry Creek reported by *Keller* [1969, 1970] found that 35 percent of the variability of the distance a bed load particle will move at the field site can be explained by the variability of the bottom velocity in the vicinity of the particle, and 68 percent can be explained by the combination of velocity and particle parameters. Keller found that on riffles movement was most influenced by differences in bottom velocity. However, particle parameters, i.e., volume, weight in water, specific gravity, and shape, are considerably more important than velocity for the movement of particles through pools. Because, velocity tends to be more uniform over the riffle, the bed velocity shows a high correlation with movement over the riffles. However at the pool cross section, two important sediment transport mechanisms occur. In the convergence zone where the near-bed velocities are highest, the significance of locally high bed velocity and shear stress is likely to be important. However, in the deeper part of the pool where bed velocities are much lower sediment mobilization is likely to rely on mobilization due to secondary circulation driven processes. In these areas, particle parameters are likely to be more significant than downstream bed shear stress as an indicator for particle movement.

[44] *Keller* [1969] reports that on Dry Creek bed material is significantly larger on bars and riffles than in the deeper parts of pools. In addition, Keller found that the large material on the point bar gradually decreases in size across the stream to the bottom of the pool. Figure 16 shows the lateral sorting of largest bed material for the pool and riffle cross sections. There is a significant peak in largest bed material at a distance of approximately 15 m. This peak in the size of the largest bed material on both the pool and riffle cross sections corresponds to the zone of maximum shear stress which is visible on Figure 9 at the higher discharges. This peak in coarsest bed material corresponds to the zone of flow convergence and supports the hypothesis that the largest bed materials are being routed around the deepest part of the pool rather than through it. This routing of sediment around the deepest part of the pools rather than through them resolves the paradox of why coarse sediment is not left in the pool on the receding discharge. *Lisle and Hilton* [1992] observed a similar mechanism with dropping stage, noting that although some fine sediment was deposited in pools, boundary shear stress along the major sediment pathways was sufficient to maintain continued transport downstream.

[45] *Lisle* [1986] has observed that both large obstructions and bends cause intense, quasi-steady secondary circulation in scour holes and goes on to suggest that "obstructions and bends are similar enough in their effects on channel form and the pattern of flow and sediment transport ... to suggest that they lie on a continuum of

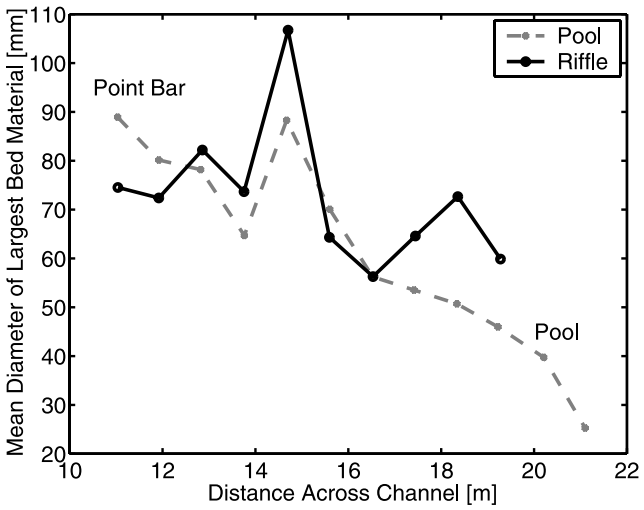

Figure 16. Lateral sorting of largest bed material size through a pool and adjacent riffle (data from *Keller* [1969]). The exact starting points for sediment sampling across the cross sections are not available, so channel distances are approximate.

bank forms affecting channel morphology." In this context, the hypothesis of flow convergence routing provides an important link with the work of *Dietrich et al.* [1979] on flow and sediment transport in meandering systems. *Dietrich et al.* [1979] found that the zone of maximum boundary shear stress is near the inside bank in the upstream bend (rather than in the deeper outside portion of the pool) and then crosses the outside bank as it enters the central segment of the bend. Similarly, the downstream velocity distribution at the upstream bend presented by *Dietrich et al.* [1979] shows a similar distribution to that predicted for the pool cross section on Dry Creek, with the highest velocities occurring over the point bar rather than the deeper part of the pool on the outside bend. *Dietrich et al.* [1979] also identified a zone of maximum sediment transport corresponding to the zone of maximum boundary shear stress and the zone of maximum particle size. This zone of coarse sediment shows a similar effect of flow convergence and sediment routing over a distinct band as is observed in the sediment distribution shown in Figure 16. As seen in Figure 9, the UnTRIM simulations predict a narrow band of high shear stress which develops downstream of the constriction at the head of the pool. The predicted shear stress distributions at discharges of 4.5 and 8.5 m^3/s show a well developed zone of high shear stress along the zone of flow convergence. At the highest discharge simulated, 17.0 m^3/s, this zone of convergence is somewhat less pronounced. As seen in Figure 9, the overall flow width at the highest discharge is more uniform and the constriction is less pronounced. This suggests the constriction may be sufficiently submerged at this discharge, whereby its influence on flow through the pool-riffle unit is reduced relative to that at lower discharges.

[46] Although the hypothesis of flow convergence routing is introduced based on the processes observed and simulated in Dry Creek, this hypothesis is consistent with observations of the significance of flow constrictions observed in other studies of pool-riffle sequences on alluvial streams [e.g., *Thompson et al.*,1998; *Booker et al.*, 2001; *Cao et al.*, 2003]. As seen in Table 1, many of the primary references pertaining to the velocity reversal hypothesis offer either stated or implied support for the hypothesis of flow convergence routing, since flow constrictions and flow convergence have been discussed in many of these references. The majority of the studies which do not directly support the flow convergence routing hypothesis are one-dimensional modeling studies, which cannot evaluate this mechanism.

[47] The model simulations presented in this study cannot directly identify the mechanisms of pool formation from a plane bed regime; however the significance of the constriction in maintaining pool-riffle morphology suggests that the presence of a constriction may also play an important role in pool formation. A study by *Lisle* [1986] found that 85% of pools were next to large obstructions or bends and that, conversely, 92% of large obstructions or bends had pools. Similarly, *Clifford* [1993b] suggested that pool-riffle units are initiated with the generation of eddies at a major flow obstacle. Further, *Clifford* [1993b] describes an autogenic process whereby the deposition downstream of a pool formed by an obstruction generates the next downstream flow irregularity. This process is consistent with the converging and diverging flow patterns fundamental to the flow convergence routing hypothesis. However, neither this study nor any of the previous studies of which we are aware rigorously track the persistence of pool-riffle sequences through time. A field reconnaissance of the Dry Creek field site in 2003 revealed that, though Keller's original pool-riffle site was still identifiable, significant incision on much of Dry Creek prohibited drawing conclusions about long-term maintenance at the site.

[48] The mechanism of flow constriction and routing observed in Dry Creek is somewhat different from the mechanism proposed by *Thompson et al.* [1996, 1998]. At their field site, *Thompson et al.* [1996, 1998] identify a constriction that blocks a portion of the channel rather than the more subtle narrowing constriction on Dry Creek. Because the channel width immediately opens up downstream of their constriction, *Thompson et al.* [1996, 1998] identify a separation zone and a recirculating eddy that form downstream of the constriction, while the primary flow is funneled into the deepest part of the pool. Although the geometry is somewhat different, the field site of *Thompson et al.* [1996] also can be explained by the hypothesis of flow convergence routing. However, in their case the flow is diverted through, rather than around, the deepest part of the pool. For this geometry, the flow convergence routing mechanism is consistent with their observations that the coarsest materials found in the pool unit are in the deepest part of the pool. *Booker et al.* [2001] identify flow routing around the deepest section of the pool for all of the pool units studied, which is identical to the flow routing observed on Dry Creek. Further, *Booker et al.* [2001] note that a recirculating eddy forms in only one of their pool units, and they suggest that the presence of recirculating zones at the pool head is a phenomenon that may act to maintain pool morphology but is of secondary importance in comparison to sediment routing. This suggests that a flow constriction is likely to be a more prominent feature in a composite hypothesis for pool-riffle morphology than the presence of

a recirculating eddy. Further consideration of the hypothesis of flow convergence routing on additional field sites is likely to yield insight into the relative importance of each of these processes on the maintenance of pool-riffle morphology in alluvial rivers.

5. Conclusions

[49] Two- and three-dimensional simulations of flow in the pool-riffle sequence on Dry Creek, CA are presented. The predicted flow velocities agree well with measured bed velocities by *Keller* [1969] and with average velocities predicted by *Keller and Florsheim* [1993] using a one-dimensional model. The model results show a reversal in mean velocity, mean near-bed velocity, maximum near-bed velocity, mean bed shear stress, and maximum bed shear stress in the pool-riffle sequence at discharges between 3.0 and 6.8 m^3/s. These results agree well with previous predictions of a reversal of bed velocity by *Keller* [1971] and a reversal in mean velocity by *Keller and Florsheim* [1993]. The application of the UnTRIM and FESWMS models to the Dry Creek pool-riffle sequence is significant because this field site served as the basis for the introduction of the velocity reversal hypothesis for pool-riffle sequences.

[50] The results of both the two-dimensional and three-dimensional simulations demonstrate that the presence of a flow constriction at the head of the pool results in a flow convergence that causes the maximum velocities to occur on the point bar of the pool rather than in the deepest part of the pool. The three-dimensional model shows a greater degree of flow and shear stress convergence and further reveals that this flow convergence drives a significant secondary circulation cell in the deepest part of the pool. It is believed that flow convergence serves to route sediment across the point bar rather than through the deepest part of the pool, while secondary circulation in the pool cross section has the potential to cause mobilization of the fine sediments in the deepest part of the pool.

[51] Though the pool-riffle sequence on Dry Creek does experience a reversal in cross-sectional average and near-bed parameters, the results presented in this study suggest that the velocity reversal hypothesis does not explain the primary mechanisms for maintaining pool-riffle morphology on Dry Creek. In light of these results that show that nonuniform flow effects are important in driving flow and sediment routing processes in the pool-riffle sequence, the velocity reversal hypothesis, which is based on cross-sectional average values, does not seem to be an adequate hypothesis to explain the important processes in maintaining pool-riffle morphology at this site. Although many studies of pool-riffle sequences have shown a convergence in mean parameters at pools and riffles, there is no evidence to suggest that a reversal in velocity must occur, and in fact many studies have shown that reversals do not occur at all pool-riffle sequences. For a hypothesis to be meaningful it must be able to explain the dominant processes; the velocity reversal hypothesis does not meet this criteria.

[52] On the basis of the processes observed on Dry Creek, the hypothesis of flow convergence routing is introduced as a new working hypothesis for defining the important processes for maintaining pool-riffle morphology in alluvial rivers. Under this hypothesis, the formation and maintenance of a pool depends on the occurrence of an upstream flow constriction which results in a convergence and acceleration of flow at the head of a pool. Flow through the pool is routed through a narrow zone within the cross section. This zone of flow routing corresponds to the highest near-bed velocities, shear stresses, maximum particle size. This zone is the primary pathway for sediment routing through or around the pool and can serve to route the coarsest sediment away from the deepest part of the pool. At the tail of the pool, the flow diverges at the head of the riffle leading to deposition on the riffle and the maintenance of a topographic high at the tail of the pool. This hypothesis is consistent with the field measurements and observations of *Keller* [1969], with the simulation results presented in this study, and with other recent studies which have identified flow constrictions as playing a major role in defining pool-riffle morphology.

[53] **Acknowledgments.** The authors would like to acknowledge Edward Keller for providing access to his unpublished data and field notebooks. The UnTRIM code was provided by V. Casulli of the University of Trento, Italy. This material is based upon work supported by National Science Foundation (grant EAR-0087842, Program Manager: L. Douglas James). Additional funding was provided to M.L.M. by a Stanford Graduate Fellowship and a NSF Graduate Research Fellowship. Financial support for this work was also provided by the U.S. Fish and Wildlife Service (contracting entity for CALFED Bay-Delta Ecosystem Restoration Program: Cooperative Agreement DCN 113322G003). We thank Edward A. Keller, Douglas M. Thompson, and an anonymous reviewer for their careful review of the manuscript and suggestions for improvements.

References

Bhowmik, N. G., and M. Demissie (1982), Bed material sorting in pools and riffles, *J. Hydraul.*, *108*, 1227–1231.

Booker, D. J., D. A. Sear, and A. J. Payne (2001), Modeling three-dimensional flow structures and patterns of boundary shear stress in a natural pool-riffle sequence, *Earth Surf. Processes Landforms*, *26*, 553–576.

Cao, Z., P. Carling, and R. Oakley (2003), Flow reversal over a natural pool-riffle sequence: A computational study, *Earth Surf. Processes Landforms*, *28*, 689–705.

Carling, P. A. (1991), An Appraisal of the velocity-reversal hypothesis for stable pool-riffle sequences in the River Severn, England, *Earth Surf. Processes Landforms*, *16*, 19–31.

Carling, P. A., and N. Wood (1994), Simulation of flow over pool-riffle topography: A consideration of the velocity reversal hypothesis, *Earth Surf. Processes Landforms*, *19*, 319–332.

Casulli, V., and P. Zanolli (2002), Semi-implicit numerical modeling of non-hydrostatic free-surface flows for environmental problems, *Math. Comput. Model.*, *36*, 1131–1149.

Celik, I., and W. Rodi (1988), Modeling suspended sediment transport in nonequilibrium situations, *J. Hydraul. Eng.*, *114*(10), 1157–1191.

Clifford, N. J. (1993a), Differential bed sedimentology and the maintenance of a riffle-pool sequence, *Catena*, *20*, 447–468.

Clifford, N. J. (1993b), Formation of riffle-pool sequences: Field evidence for an autogenetic process, *Sediment. Geol.*, *85*, 39–51.

Clifford, N. J., and K. S. Richards (1992), The reversal hypothesis and the maintenance of riffle-pool sequences: A review and field appraisal, in *Lowland Floodplain Rivers: Geomorphological Perspectives*, edited by P. A. Carling and G. E. Petts, pp. 43–70, John Wiley, Hoboken, N. J.

Dietrich, W. E., J. D. Smith, and T. Dunne (1979), Flow and sediment transport in a sand bedded meander, *J. Geol.*, *87*, 305–315.

Froehlich, D. C. (1989), Finite element surface-water modeling system: Two-dimensional flow in a horizontal plane-users manual, *Rep. FHWA-RD-88–177*, 285 pp., Fed. Highway Admin., Washington, D. C.

Gilbert, G. K. (1914), The transportation of debris by running water, *U.S. Geol. Surv. Prof. Pap.*, *86*.

Jackson, W. L., and R. L. Beschta (1982), A model of two-phase bedload transport in an Oregon coast range stream, *Earth Surf. Processes Landforms*, *7*, 517–527.

Keller, E. A. (1969), Form and fluvial processes of Dry Creek, near Winters, California, M.S. thesis, Univ. of Calif., Davis.

Keller, E. A. (1970), Bed-load movement experiments: Dry Creek, California, *J. Sediment. Petrol.*, *40*, 1339–1344.

Keller, E. A. (1971), Areal sorting of bed-load material: The hypothesis of velocity reversal, *Geol. Soc. Am. Bull.*, *82*, 753–756.

Keller, E. A. (1972), Development of alluvial stream channels: A five stage model, *Geol. Soc. Am. Bull.*, *83*, 1531–1536.

Keller, E. A., and J. L. Florsheim (1993), Velocity-reversal hypothesis: A model approach, *Earth Surf. Processes Landforms*, *18*, 733–740.

Kieffer, S. W. (1985), The 1983 hydraulic jump in Crystal Rapid: Implications for river-running and geomorphic evolution in the Grand Canyon, *J. Geol.*, *93*, 385–406.

Kieffer, S. W. (1989), Geologic nozzles, *Rev. Geophys.*, *27*, 3–38.

Lisle, T. (1979), A sorting mechanism for a riffle-pool sequence, *Geol. Soc. Am. Bull., Part II*, *90*, 1142–1157.

Lisle, T. E. (1986), Stabilization of a gravel channel by large streamside obstructions and bedrock bends, Jacoby Creek, northwest California, *Geol. Soc. Am. Bull.*, *97*, 999–1011.

Lisle, T. E., and S. Hilton (1992), The volume of fine sediment in pools: An index of sediment supply in gravel-bed streams, *Water Resour. Bull.*, *28*, 371–383.

MacWilliams, M. L. (2004), Three-dimensional hydrodynamic simulation of river channels and floodplains, Ph.D. dissertation, 222 pp., Stanford Univ., Stanford, Calif.

Miller, A. J. (1994), Debris-fan constrictions and flood hydraulics in river canyons: Some implications from two-dimensional flow modelling, *Earth Surf. Processes Landforms*, *19*, 681–697.

Pasternack, G. B., C. L. Wang, and J. E. Merz (2004), Application of a 2D hydrodynamic model to design of reach-scale spawning gravel replenishment on the Mokelumne River, California, *River Res. Appl.*, *20*, 202–225.

Petit, F. (1987), The relationship between shear stress and the shaping of the bed of a pebble-loaded river La Rulles–Ardenne, *Catena*, *14*, 453–468.

Petit, F. (1990), Evaluation of grain shear stresses required to initiate movement of particles in natural rivers, *Earth Surf. Processes Landforms*, *15*, 135–148.

Richards, K. S. (1978), Simulation of flow geometry in a riffle-pool stream, *Earth Surf. Processes*, *3*, 345–354.

Rodi, W. (1993), *Turbulence Models and Their Application in Hydraulics: A State-of-the-Art Review*, 3rd ed., A. A. Balkema, Brookfield, Vt.

Schmidt, J. C. (1990), Recirculating flow and sedimentation in the Colorado River in Grand Canyon, Arizona, *J. Geol.*, *98*, 709–724.

Schmidt, J. C., D. M. Rubin, and H. Ikeda (1993), Flume simulation of recirculating flow and sedimentation, *Water Resour. Res.*, *29*, 2925–2939.

Sear, D. A. (1996), Sediment transport processes in pool-riffle sequences, *Earth Surf. Processes Landforms*, *21*(3), 241–262.

Shewchuk, J. R. (1996), Triangle: Engineering a 2D quality mesh generator and Delaunay triangulator, in *Applied Computational Geometry: Towards Geometric Engineering*, vol. 1148, edited by M. C. Lin and D. Manocha, pp. 203–222, Springer, New York.

Thompson, D. M. (2004), The influence of pool length on local turbulence production and energy slope: A flume experiment, *Earth Surf. Processes Landforms*, *29*, 1341–1358.

Thompson, D. M., E. E. Wohl, and R. D. Jarrett (1996), A revised velocity-reversal and sediment sorting model for a high-gradient, pool-riffle stream, *Phys. Geogr.*, *17*(2), 142–156.

Thompson, D. M., J. M. Nelson, and E. E. Wohl (1998), Interactions between pool geometry and hydraulics, *Water Resour. Res.*, *34*(12), 3673–3681.

Thompson, D. M., E. E. Wohl, and R. D. Jarrett (1999), Velocity reversals and sediment sorting in pools and riffles controlled by channel constrictions, *Geomorphology*, *27*, 229–241.

Whiting, P. J., and W. E. Deitrich (1991), Convective accelerations and boundary shear stress over a channel bar, *Water Resour. Res.*, *27*(5), 783–796.

P. K. Kitanidis, R. L. Street, and M. L. MacWilliams Jr., Environmental Fluid Mechanics Laboratory, Department of Civil and Environmental Engineering, Stanford University, Stanford, CA 94305-4020, USA. (mmacwill@stanford.edu)

G. B. Pasternack and J. M. Wheaton, Department of Land, Air, and Water Resources, University of California, Davis, 1 Shields Avenue, Davis, CA 95616-8626, USA.